

VI

Axially Loaded Members

VI.1 Introduction

A slender member which has a straight axis in the undeformed configuration, is said to be under purely axial loading if that axis remains a straight line after deformation, which may be caused by a constant axial force or other symmetrical actions, such as a uniform temperature variation. According to this definition and to the law of conservation of plane sections, in a prismatic bar under purely axial loading, any two cross-sections remain parallel after the deformation, i.e., only the distance between them varies.

Considering, in a prismatic bar under purely axial loading, two cross-sections at a distance l from each other in the undeformed bar, this distance will change to a value l' after the deformation and the strain defined by the variation of that distance is given by the expression

$$\varepsilon = \frac{l' - l}{l} . \quad (113)$$

This strain is constant in the cross-section. Therefore, if the bar is homogeneous, i.e., if it is made of a material with the same rheological properties in the whole member, the stress σ will also be constant. The position of the resultant of the system of forces defined by the stresses acting in the cross-section may be obtained by computing the moment of the stresses in relation to any axis of the cross-section's plane, which must be equal to the moment of the resultant in relation to the same axis (Fig. 59). The moment of the force acting in the infinitesimal area $d\Omega$, $dN = \sigma d\Omega$, is $dM = dN x = \sigma d\Omega x$. Integrating this expression to the whole area Ω of the cross-section gives the moment of the stresses. This moment must be equal to the moment of the resultant axial force $N = \sigma \Omega$, which takes the value $N d = \sigma \Omega d$. The distance d of the resultant to the reference axis r (Fig. 59) is then

$$\int_{\Omega} \sigma x d\Omega = \sigma \Omega d \Rightarrow d = \frac{\int_{\Omega} x d\Omega}{\Omega} . \quad (114)$$

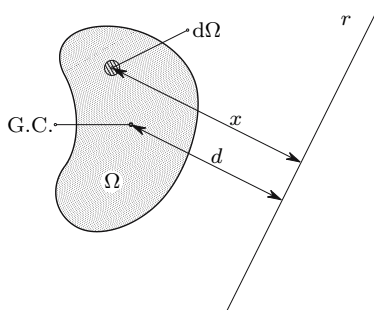


Fig. 59. Determination of the position of the stress resultant in the cross section of a slender member under purely axial loading

Equation (114) is also the expression used to compute the position of the center of gravity or centroid of a plane area Ω . Thus, we may conclude that *in a homogeneous prismatic bar under purely axial loading the line of action of the resultant of the applied forces contains the centroid of the cross-section.*

VI.2 Dimensioning of Members Under Axial Loading

If the axial force is tensile, the cross-section area Ω must be given dimensions which lead to a nominal value of the acting stress σ_{Ed} that is smaller than the nominal value of the material's resisting stress (allowable stress) σ_{all} . This condition may be expressed by the inequality

$$\sigma_{Ed} = \frac{N_{Ed}}{\Omega} \leq \sigma_{all} \Rightarrow \Omega \geq \frac{N_{Ed}}{\sigma_{all}}, \quad (115)$$

where N_{Ed} represents the nominal value of the axial force. In the following exposition the indices "Ed" of the acting forces and stresses are omitted, i.e., the values of internal or external forces and stresses written without indices are nominal values.

In compressed members (115) is a necessary but not a sufficient condition, since the phenomenon of *buckling* may occur. This kind of problems is analysed in Chap. XI. In this chapter we consider that the stability of the compressed member is guaranteed.

VI.3 Axial Deformations

As seen above, in a bar under pure axial loading the stress state may be considered as uniform, irrespective of how the forces are applied, provided that the material points under consideration are not close to the region of the member where the forces are applied (Saint-Venant's principle). In axially

loaded slender members these regions are generally a small part of the member, so that a uniform distribution of the stresses may be accepted when the elongation of the bar is computed.

In the case of a material with linear elastic rheological behaviour the elongation Δl is given by the expression (cf. (113))

$$\Delta l = l' - l = \varepsilon l = \frac{\sigma}{E} l = \frac{Nl}{E\Omega}, \quad (116)$$

where l and l' represent the length of the bar, before and after the deformation, respectively. The quantity $E\Omega$ represents the *axial stiffness*, since the larger this value, the smaller the member's deformation caused by the axial force.

If, in addition to the axial force a uniform temperature variation ΔT occurs, the total elongation may be computed by the expression

$$\Delta l = \left(\frac{N}{E\Omega} + \alpha\Delta T \right) l, \quad (117)$$

where α represents the *coefficient of thermal expansion* of the material.

VI.4 Statically Indeterminate Structures

VI.4.a Introduction

Statically determinate structures are freely deformable, in the sense that their supports and internal connections do not restrict the deformations. This means that a small change in the geometry or size of the structural elements does not change the distribution of internal forces. For example, if the length of the left bar of the plane truss represented in Fig. 60-a increases Δl (e.g., due to a temperature increase), the truss adapts its geometry without the need of internal forces.

In the statically indeterminate structure represented in Fig. 60-b, however, there can be no change in the length of one of the bars without altering the

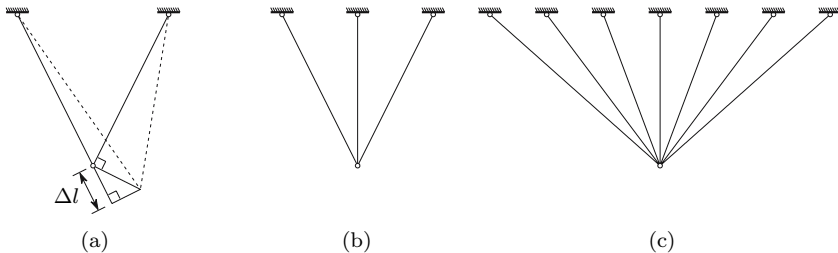


Fig. 60. Examples of structures with the same degree of kinematic indeterminacy and different degrees of statical indeterminacy

lengths of the other two: if, for example, the middle bar suffers a temperature increase, the three bars can only remain connected if the middle bar is compressed and the lateral bars are stretched, which requires tensile axial forces.

A statically determinate structure only has internal forces if external forces are applied, which means that they are insensitive to temperature change, material retraction, or any other actions that alter the dimensions of structural elements. Statically indeterminate structures, on the other hand, may have internal forces in the absence of external forces, as seen in the example above. Nevertheless, in these structures the release of a connection (for example, by the yielding or rupture of one bar) does not necessarily imply structural collapse, as statically indeterminate structures have a number of connections, which is greater than the minimum necessary to guarantee the static equilibrium.

VI.4.b Computation of Internal Forces

Since in statically indeterminate structures the internal forces are not independent of the deformation of structural elements, *conditions of compatibility of the deformations* must be taken in account in order to compute the internal forces. There are two main general methods to establish these conditions:

- *Direct*, by first releasing a number of connections equal to the degree of static indeterminacy, and then computing the displacements which appear in the released connections (these displacements are zero in the real structure) and the forces necessary to eliminate these displacements. Taking as an example the truss represented in Fig. 60-b, the vertical restriction of the middle support, for example, may be released. The vertical displacement of the upper end of the middle bar (caused by external forces, temperature, etc.) is then computed. The force needed to cause a displacement in the opposite direction, i.e., to bring the upper end of the middle bar back to the initial position, corresponds to the vertical reaction force of the middle support. This force is the *hyperstatic unknown* or *redundant force*. Once this force is computed, the remaining reaction and internal forces may be obtained by means of static equilibrium considerations. This method is known as *the force method*, since the unknowns are the forces acting on the connections which were released in the first computation step.
- *Indirect*, taking as unknowns the displacements necessary to define fully the deformed configuration of the structure. These displacements – the *kinematic unknowns* – are computed by establishing the relations between them and the resultants of the internal forces in a deformed configuration. The conditions of equilibrium between these resultants and the external forces gives a system of equations, whose solution yields the unknown displacements. Once these displacements are known, all the internal forces may be computed. This method is known as *the displacement method*, as the

unknowns are displacements. The displacement method is more easily generalized to structures with non-linear behaviour than the force method.

The number of equations to be solved corresponds to the *degree of static indeterminacy* for the force method and to the *degree of kinematic indeterminacy* in the case of the displacement method. These two quantities are not related. For example, all the three trusses represented in Fig. 60 have a degree of kinematic indeterminacy of two (the two components of the displacement vector in the connection node of the bars) and degrees of static indeterminacy of zero, one and five, respectively. The detailed study of these two methods and their systematization belong to the scope of the Theory of Structures. Here they are only applied to simple structures in a general form.

VI.4.c Elasto-Plastic Analysis

The rheological behaviour of materials which display a well-defined yielding zone, such as mild steel, may be approximated by the idealized constitutive law represented in Fig. 61, provided that the strain does not reach the hardening zone (cf. Fig. 47). As seen in Sect. IV.3, such a rheological behaviour is called elastic, perfectly plastic.

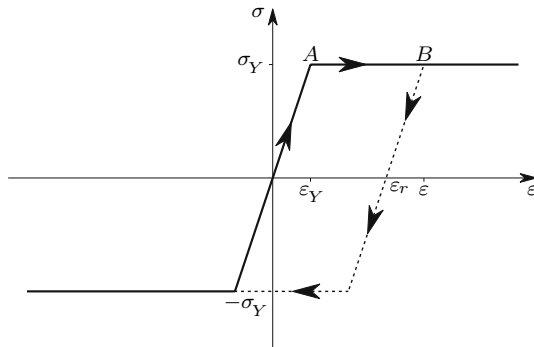


Fig. 61. Elastic, perfectly plastic rheological behaviour

The strain fraction corresponding to the yielding zone is generally much larger than the maximum elastic strain ε_Y . In mild steel, for example, yielding starts with a strain of approximately 0.1% and hardening starts with $\varepsilon \approx 1.5\%$. The yielding zone in this case is 14 times the maximum elastic strain. Thus, in a structure made of a ductile material with a yielding zone, we usually admit that in the structural elements where the yielding stress is first attained the stress keeps this value until collapse, unless there is a decrease in deformation, as defined by the constitutive law represented in Fig. 61.

Despite these simplifying assumptions, the computation of structures in the elasto-plastic range is substantially more complex than in the linear case.

The superposition principle is not valid any longer and the order of application of the external forces must be taken into account, as well as the different material behaviour when the strain changes from the elastic to the plastic range or vice versa.

To illustrate these considerations the elasto-plastic behaviour of the hyperstatic truss represented in Fig. 62 is described in detail. In order to keep the description as simple as possible, we assume that the three bars have equal cross-section areas Ω and that the material behaviour follows the simplest elasto-plastic constitutive law, as represented in Fig. 61. The displacement method is used for the analysis.

The conditions of static equilibrium are valid in any range (elastic, elasto-plastic or plastic). As a consequence of the symmetry of geometry and loading, only the vertical condition of equilibrium needs to be considered, yielding the relation

$$P = N_1 + 2N_2 \cos 60^\circ \Rightarrow P = N_1 + N_2 . \quad (118)$$

The deformation's conditions of compatibility, when expressed in terms of displacements and strains are also valid in any range. In the present case the degree of kinematic indeterminacy is one, since the deformed configuration of the structure is completely defined by the vertical displacement of the point of application of load P . Denoting this displacement by δ (Fig. 62) and considering that it is sufficiently small to be considered as infinitesimal, the relation between δ and the strains in the bars is given by (119) (the dashed lines represent the deformed configuration with largely exaggerated displacements)

$$\delta = \Delta l_1 = \frac{\Delta l_2}{\cos 60^\circ} \Rightarrow \varepsilon_1 l = \frac{\varepsilon_2 \frac{l}{\cos 60^\circ}}{\cos 60^\circ} \Rightarrow \varepsilon_1 = 4\varepsilon_2 , \quad (119)$$

since, in the case of infinitesimal rotations, the arcs of circumference used to draw the undeformed length of bars 2 on the dashed lines may be substituted by the normals to those lines (Fig. 62). ε_1 and ε_2 represent the strains in bars 1 and 2, respectively.

If the deformations are caused only by the axial force, i.e., in absence of plastic deformations, temperature variation, residual strains, etc., the condition of compatibility may be expressed in terms of the axial forces, N_1 and

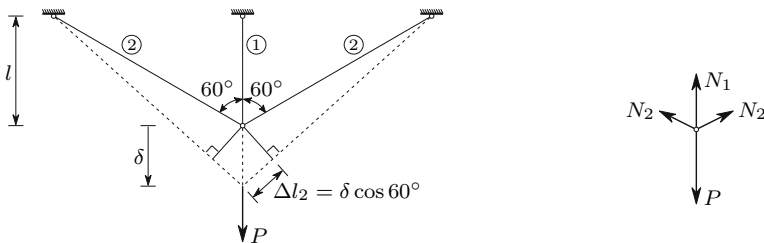


Fig. 62. Conditions of equilibrium and compatibility

N_2 , by the equation

$$\delta = \frac{N_1 l}{E\Omega} = 4 \frac{N_2 l}{E\Omega} \Rightarrow N_1 = 4N_2, \quad (120)$$

Next the internal forces and the displacement δ in the different loading stages are analysed.

- *Elastic phase.* In this stage the axial forces may be computed by solving the system of two equations described by (118) and (120), yielding

$$\begin{cases} N_1 = \frac{4}{5}P \\ N_2 = \frac{1}{5}P \end{cases} \Rightarrow \delta = \frac{4}{5} \frac{l}{E\Omega} P \Rightarrow K_1 = \frac{\partial P}{\partial \delta} = \frac{5}{4} \frac{E\Omega}{l}, \quad (121)$$

where K_1 represents the structural stiffness corresponding to the displacement δ .

Since the strain ε_1 is always superior to the strain in bar 2 (119), bar 1 reaches the yielding strain at first. The values of the loading P and displacement δ corresponding to the yielding of bar 1 may be obtained from (121) and (120), taking the values

$$\begin{aligned} \sigma &= \sigma_Y \Rightarrow N_1 = N_{1Y} = \Omega\sigma_Y \\ \Rightarrow P &= P_1 = \frac{5}{4}\Omega\sigma_Y \Rightarrow \delta = \delta_1 = \frac{\sigma_Y l}{E}. \end{aligned} \quad (122)$$

- *Elasto-plastic phase.* When the load P exceeds the value P_1 , the axial force in bar 1 remains constant, with the value N_{1Y} , since the strain is in the yielding zone. As this internal force is known, the structure becomes statically determinate. Thus, the axial force N_2 may be obtained directly from the equilibrium condition (118), yielding

$$P = N_{1Y} + N_2 \Rightarrow N_2 = P - \Omega\sigma_Y \quad \text{with } P > P_1. \quad (123)$$

Taking in consideration that the lateral bars are still in the elastic range, the first of (120) may be used to compute the displacement and stiffness in the elasto-plastic phase, yielding

$$\delta = \frac{4N_2 l}{E\Omega} = (P - \Omega\sigma_Y) \frac{4l}{E\Omega} \Rightarrow K_2 = \frac{\partial P}{\partial \delta} = \frac{1}{4} \frac{E\Omega}{l} = \frac{1}{5} K_1. \quad (124)$$

The structure collapses (yielding of the three bars) when the lateral bars reach the yielding strain. From (123), (122) and (124) we get

$$N_2 = N_{2Y} = \Omega\sigma_Y \Rightarrow \begin{cases} P = P_Y = 2\Omega\sigma_Y = \frac{8}{5} \frac{5}{4} \Omega\sigma_Y = \frac{8}{5} P_1 \\ \delta = \delta_Y = 4 \frac{\sigma_Y l}{E} = 4\delta_1. \end{cases} \quad (125)$$

At the moment of collapse the strain in bar 1 is therefore four times the yielding strain of the material, $\varepsilon_Y = \frac{\sigma_Y}{E}$, and the corresponding load P_Y is $\frac{8}{5}$ times the maximum load in the elastic range. Assuming the structure is made of mild steel, bar 1 is still at the beginning of the yielding zone when the structure collapses.

If the structure is unloaded in the elasto-plastic phase, the middle bar, which has already suffered some plastic deformation, has an elastic behaviour in the unloading, but has a residual strain $\varepsilon_{1r} = \varepsilon_{1\max} - \frac{\sigma_Y}{E}$ ($\varepsilon_{1\max}$ is the maximum value of the strain in the loading phase), as represented in Fig. 61 (dashed line). Let us now analyse the behaviour of the structure, as a function of this residual strain. The strain in bar 1 is now given by

$$\varepsilon_1 = \frac{N_1}{E\Omega} + \varepsilon_{1r} .$$

From this relation and the compatibility condition (119), we get

$$\varepsilon_1 = 4\varepsilon_2 \Rightarrow \frac{N_1}{E\Omega} + \varepsilon_{1r} = 4 \frac{N_2}{E\Omega} \Rightarrow N_1 = 4N_2 - E\Omega\varepsilon_{1r} .$$

This expression and the equilibrium condition (118) define a system of equations which allows the computation of the axial forces N_1 and N_2 , yielding

$$\left\{ \begin{array}{l} N_1 = \frac{4}{5}P - \frac{1}{5}E\Omega\varepsilon_{1r} \\ N_2 = \frac{1}{5}P + \frac{1}{5}E\Omega\varepsilon_{1r} \end{array} \right. \Rightarrow \left\{ \begin{array}{l} \delta = 4\varepsilon_2 l = 4 \frac{N_2}{E\Omega} l = \frac{4}{5} \frac{l}{E\Omega} P + \frac{4}{5} l \varepsilon_{1r} \\ \Rightarrow K_3 = \frac{\partial P}{\partial \delta} = \frac{5}{4} \frac{E\Omega}{l} = K_1 . \end{array} \right. \quad (126)$$

From this expression we verify that, in the unloading, the stiffness of the structure is equal to the stiffness in the initial elastic phase. This is a consequence of having all bars in the elastic phase.

Equation (126) remain valid while the middle bar has the residual strain ε_{1r} and the lateral bars are in the elastic phase. This situation changes only if P exceeds the value which caused the the residual strain ε_{1r} in the loading phase ($P = P_{\max}$, Fig. 63), or if bar 1 attains the compressive yielding stress ($\sigma = -\sigma_Y$, Fig. 61). The value of P corresponding to the last situation may be computed by means of the axial force in the middle bar, expressed as a function of the maximum value of P in the loading phase P_{\max} ($P_1 < P_{\max} < P_Y$). From (124) we get

$$\varepsilon_{1\max} = \frac{\delta_{\max}}{l} = 4 \frac{P_{\max} - \Omega\sigma_Y}{E\Omega} \Rightarrow \varepsilon_{1r} = \varepsilon_{1\max} - \frac{\sigma_Y}{E} = 4 \frac{P_{\max}}{E\Omega} - 5 \frac{\sigma_Y}{E} . \quad (127)$$

Substituting this value of ε_{1r} in the first of (126), we get

$$N_1 = \Omega\sigma_Y - \frac{4}{5} (P_{\max} - P) . \quad (128)$$

Bar 1 attains the compressive yielding stress, when the axial force N_1 reaches the value $N_1 = -\Omega\sigma_Y$. From this condition and from (128) we get, considering the value of P_1 given by (122),

$$N_1 = -\Omega\sigma_Y \Rightarrow P = P_4 = P_{\max} - \frac{5}{2}\Omega\sigma_Y = P_{\max} - 2P_1. \quad (129)$$

If the maximum value of P in the loading phase is P_1 , the middle bar yields in compression for $P_4 = -P_1$, as might be expected, since no residual deformations were caused in the loading phase and the material has the same behaviour for tensile and compressive stresses. However, if a tensile plastic deformation takes place in bar 1, which happens in the above-described elasto-plastic phase ($P_1 < P_{\max} < P_Y$), there is a residual elongation of bar 1. As a consequence, the structural behaviour for the positive and negative values of P becomes different ($P_4 \neq -P_1$).

The behaviour of the structure in the different loading stages analysed above may be summarized by the force-displacement (P - δ) diagram presented in Fig. 63. In this diagram the line $OABC$ represents the load-displacement relation in a first loading. Line \overline{OA} represents the elastic phase, line \overline{AB} the elasto-plastic phase (the middle bar is in the yielding zone and the lateral bars are still in linear-elastic regime) and line \overline{BC} the plastic stage (structural yielding or collapse). Line $OGHI$ represents the structural behaviour in a first loading with negative values of the force P .

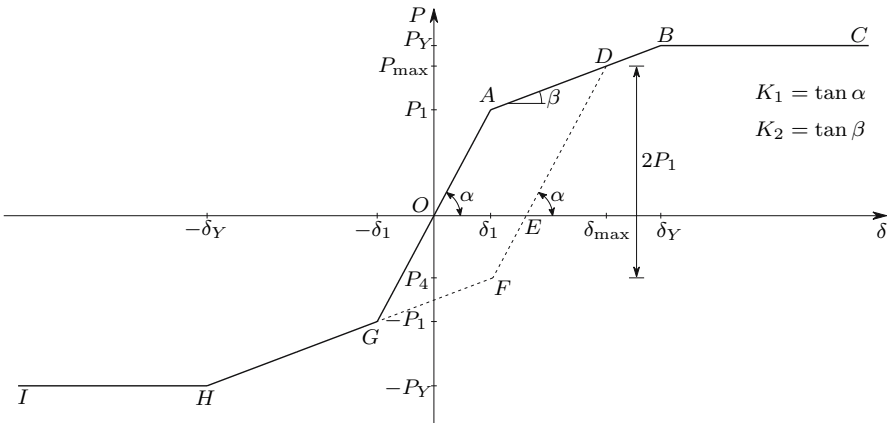


Fig. 63. Load-displacement diagram of the truss represented in Fig. 62

The structural behavior in the unloading from a load P_{\max} in the elasto-plastic phase is described by the line \overline{DE} which is parallel to line \overline{OA} , as seen above (same structural stiffness: $K_3 = K_1$, (126)). If, after unloading from P_{\max} (point E), a negative load is applied (reversed force P), the structure behaves elastically until point F , which represents the yielding of the middle

bar in compression (129). Yielding of the lateral bars under compression takes place for a displacement $\delta = -\delta_Y$ (point H), since the load P_{\max} did not cause yielding of these bars, which means that its behaviour is the same as in a first compressive loading (line $OGHI$).

In the reloading from any point of line FD the structure follows the line $EDBC$, since at point D the structure re-enters in the elasto-plastic phase, with a strain in the middle bar of $\varepsilon_1 = \varepsilon_{1r} + \frac{\sigma_Y}{E}$ ((127) and Fig. 61, point B).

In comparison with the first loading, the behaviour of the structure in the reloading, which is represented by lines $EDBC$ and $EFGHI$ for positive and negative values of P , respectively, shows an increase of the elastic loading capacity (hardening: $P_{\max} > P_1$) for positive values of P (line ED) and softening (reduction of the elastic loading capacity: $|P_4| < |P_1|$) for negative values (line EF).

The hardening for positive loads is accompanied by a reduction of the deformation capacity. Conversely, for negative P -values, softening and increase of the deformation capacity took place (horizontal projection of $EFGHI$).

There is an analogy between the behaviour of this structure and the strain hardening process of steel described in Sect. V.5. In fact, in both cases the pre-deformation introduced by tensile forces increases the tensile elasticity limit and the deformation capacity in compression and vice versa for a compressive pre-deformation. The structure represented in Fig. 62 may therefore be seen as a *physical model* for the strain hardening process of ductile materials. Figure 64 gives two other models. The second one includes a yielding zone. In this figure the numbered corners in the diagrams represent a starting yielding of the corresponding bars. In unloading followed by a reloading, model a follows the dashed line which is parallel to line $\overline{O\bar{I}}$. Model b also has an elastic behaviour in the unloading, which, however, is more complex than in the case of model a . The analysis of the unloading in model b is left as an exercise for the reader.

VI.5 An Introduction to the Prestressing Technique

Let us consider now that the truss represented in Fig. 62 is made of a brittle material with linear elastic behaviour until rupture, which occurs when the stress attains the value σ_r . In order to make the comparisons easier, let us consider $\sigma_r = \sigma_Y$. Expressions 121 are still valid for representing the load-displacement relation, since, in the elastic phase, the only material parameter needed is the elasticity modulus E . However, when P reaches the value which causes the rupture of the middle bar, $P = P_r = \frac{5}{4}\Omega\sigma_r = \frac{5}{4}N_r$ ((122); N_r is the rupture load of a bar), the structure collapses totally. In fact, the loading capacity of the lateral bars alone is not sufficient to sustain the load P_r , as can be easily verified by the condition of equilibrium

$$P = 2N_2 \cos 60^\circ \Rightarrow N_2 = P_r = \frac{5}{4}N_r > N_r .$$

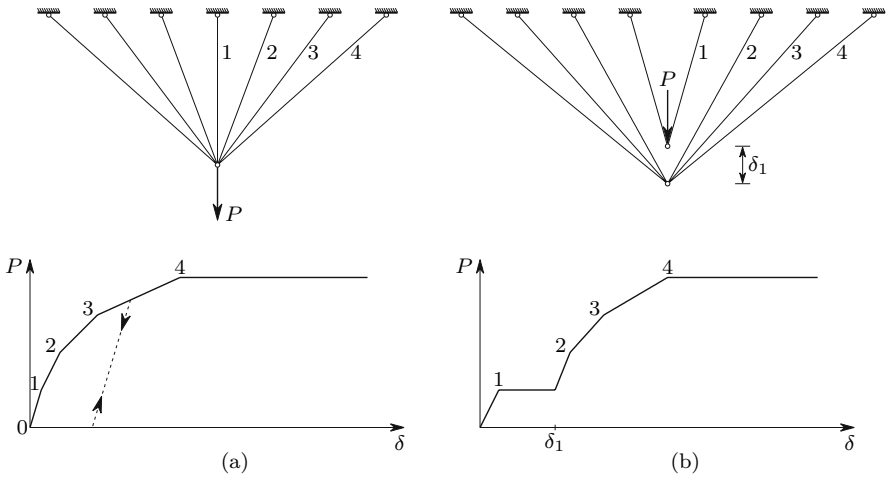


Fig. 64. Physical models for the behaviour of a ductile material with hardening (a) without yielding zone; (b) with yielding zone

This example shows that the strength reserves of a ductile structure, in relation to the load causing the first plastic deformations ($P_Y > P_1$ in the ductile truss, Fig. 63), may not exist if the structure is made of a brittle material.

However, the loading capacity of the brittle structure may also be increased, by introducing *prestressing* residual forces. In order to introduce this technique, let us assume that the undeformed middle bar does not have exactly the length l , but is slightly longer, with a length $l + l_r$. Under these conditions the three bars can only be connected, if the middle bar is compressed, which introduces tensile axial forces in the lateral bars. This means that the structure will have residual internal forces, i.e., the internal forces will not be zero, when the external forces vanish. In the analysis of the structure l_r may be treated as a residual elongation. Thus, the structural behaviour may be defined by (126), if ε_{1r} is substituted by $\frac{l_r}{l}$, yielding

$$\left\{ \begin{array}{l} N_1 = \frac{4}{5}P - \frac{1}{5} \frac{E\Omega l_r}{l} \\ N_2 = \frac{1}{5}P + \frac{1}{5} \frac{E\Omega l_r}{l} \end{array} \right. \Rightarrow \delta = \frac{4}{5} \frac{l}{E\Omega} P + \frac{4}{5} l_r \Rightarrow K = \frac{\partial P}{\partial \delta} = \frac{5}{4} \frac{E\Omega}{l}. \quad (130)$$

The maximum loading capacity of the structure is achieved if the three bars reach the rupture stress simultaneously, as may be easily concluded from the equilibrium condition (118). This means that, at the collapse, we have $N_1 = N_2 = \Omega\sigma_r$. Introducing this condition in the first of (130), we get

$$\begin{cases} \frac{4}{5}P - \frac{1}{5}\frac{E\Omega l_r}{l} = \Omega\sigma_r \\ \frac{1}{5}P + \frac{1}{5}\frac{E\Omega l_r}{l} = \Omega\sigma_r \end{cases} \Rightarrow \begin{cases} P = 2\Omega\sigma_r \\ l_r = \frac{3l\sigma_r}{E} \end{cases} . \quad (131)$$

From this result we conclude that the optimal prestressing is obtained by a residual elongation $l_r = \frac{3l\sigma_r}{E}$, which increases the loading capacity of the structure from $\frac{5}{4}\Omega\sigma_r$ to $2\Omega\sigma_r$. The displacement δ just before the collapse, taking as reference configuration the structure without prestressing, i.e., when the vertical distance between the connection node and the middle support is exactly l , may be obtained from the elongation of the lateral bars, since they have a zero axial force for $\delta = 0$ (reference configuration). Thus, we obtain from (119)

$$\varepsilon_2 = \frac{\sigma_r}{E} \Rightarrow \delta = 4\varepsilon_2 l = 4\frac{\sigma_r l}{E} .$$

We conclude that, if the brittle and ductile structures have the same elasticity modulus E and ultimate stress $\sigma_r = \sigma_Y$, the deformation of the brittle structure at the rupture takes the same value as the deformation of the ductile structure when yielding starts (δ_Y , (125)).

The initial internal forces caused by the prestressing may be obtained from (130), by taking $P = 0$ and $l_r = 3l\frac{\sigma_r}{E}$, yielding

$$N_1 = -N_2 = \frac{3}{5}\Omega\sigma_r = \frac{3}{5}N_r .$$

In this case the initial axial forces are lower than the loading capacity of the bars. However, it very often happens that *minimum loads* are required in prestressed structures, in order to prevent the initial loads causing failure of structural elements (cf. Example VI.10).

These two examples (ductile and brittle structure of Fig. 62) illustrate the fundamental differences in the behaviour of structures made of ductile and brittle materials:

- In ductile structures, a *redistribution of the internal forces* takes place automatically, which alters the relations between the internal forces in the different elements and allows the most strained elements to keep their loading capacity until the structure collapses. In the example, the middle bar keeps its loading capacity until the lateral bars reach the yielding axial force.¹
- In brittle structures, the full loading capacity of the structural elements can only be used by means of prestressing residual forces. The prestressing technique must be implemented in a carefully controlled way, since small changes in the prestressing parameters (in the example parameter l_r), caused by temperature differences, creep, shrinkage, etc., may cause

¹If the ductile structure is prestressed with $l_r = \frac{3l\sigma_r}{E}$ (131) the three bars reach the yielding strain simultaneously.

substantial changes in the loading capacity of the structure. Furthermore, the increase of loading capacity only takes place for the loading case under consideration: in the example, the prestressing considered causes a decrease in the compressive loading capacity of the structure. The above-mentioned minimum loads may also be a drawback of prestressed structures.

From the above considerations we may conclude that ductile structures are safer, since their capacity for internal force redistribution makes them less sensitive to imperfections and construction errors, and also because their failure does not happen unannounced, since it is usually preceded by large plastic deformations.

VI.6 Composite Members

VI.6.a Introduction

In prismatic bars made of two or more materials, with a constant cross-section, the law of conservation of plane sections remains valid, since the symmetry conditions in relation to the cross-section's plane still hold (Fig. 58). As a consequence, in the case of purely axial loading, the strain is constant in the cross-section. However, as the material is not the same throughout the cross-section, the stresses will not be constant and will depend on the rheological properties of the materials. We therefore have a statically indeterminate problem, which means that we may have internal forces without external loads, caused, for example, by a temperature variation. The degree of static indeterminacy is equal to the number of materials minus one. The forces in the connections between the different materials may be considered as the hyperstatic unknowns. The degree of kinematic indeterminacy is one, regardless of the number of materials. The strain in the cross-section may be taken as the kinematic unknown, since, once it is known, the stresses in all materials may be computed directly.

In the present analysis the displacement method will be used. For the sake of simplicity, members made of two linear elastic materials are considered. The generalization of the analysis to any number of materials is straightforward (cf. Example VI.14)

VI.6.b Position of the Stress Resultant

In a prismatic bar under purely axial loading the strain ε is constant in the cross-section, as shown above. The stresses in materials a and b are then $\sigma_a = E_a \varepsilon$ and $\sigma_b = E_b \varepsilon$,² where E_a and E_b represent the Young's moduli of materials a and b , respectively. By using the same line of reasoning as

²If the Poisson's coefficients in the two materials are different, the axial loading will generally cause stresses in longitudinal facets, since the transversal deforma-

for homogeneous members (Fig. 59) and denoting by Ω_a and Ω_b the areas occupied by the two materials in the cross-section, we get

$$\begin{aligned} \overbrace{\int_{\Omega_a} \sigma_a x \, d\Omega_a + \int_{\Omega_b} \sigma_b x \, d\Omega_b}^{\text{moment of the stresses}} &= \overbrace{(\sigma_a \Omega_a + \sigma_b \Omega_b) d}^{\text{moment of the axial force}} \\ \Rightarrow d &= \frac{E_a \int_{\Omega_a} x \, d\Omega_a + E_b \int_{\Omega_b} x \, d\Omega_b}{E_a \Omega_a + E_b \Omega_b}. \end{aligned} \quad (132)$$

Thus, the axial force will not cause bending, i.e., the axis of the bar will remain a straight line, if its line of action contains the point defined by two distances d , computed by means of (132), considering two non-parallel reference axes of the cross-section's plane. This expression also defines the position of the section's centroid, *if the area occupied by each material is weighted with its Young's modulus*. A fundamental difference between this expression and (114) is that the latter does not depend on the material behaviour, as opposed to this one, which *is only valid for materials with linear elastic behaviour*.

VI.6.c Stresses and Strains Caused by the Axial Force

As explained in Sect. VI.6.a, the determination of stresses in composite members is a statically indeterminate problem, since a condition of deformation compatibility must be taken into account. In the case of purely axial loading that condition is represented by the relation $\varepsilon_a = \varepsilon_b \Rightarrow \frac{\sigma_a}{E_a} = \frac{\sigma_b}{E_b}$, as seen in the previous section. The last of these relations and the equilibrium condition $N = \sigma_a \Omega_a + \sigma_b \Omega_b$ define a system of two equations, whose solution yields the stresses in the two materials

$$\begin{cases} \sigma_a = \frac{N}{E_a \Omega_a + E_b \Omega_b} E_a \\ \sigma_b = \frac{N}{E_a \Omega_a + E_b \Omega_b} E_b \end{cases} \Rightarrow \begin{cases} \sigma_a = \frac{N}{\Omega_a + m_a \Omega_b} \\ \sigma_b = \frac{N}{m_b \Omega_a + \Omega_b} \end{cases}. \quad (133)$$

In the last expressions $m_a = \frac{E_b}{E_a}$ and $m_b = \frac{E_a}{E_b}$ are called *homogenizing coefficients*, which allow the computation of the stresses in almost the same way, as in the case of homogeneous sections. For example, the stress in material a may be obtained by considering the cross-section area obtained by multiplying the

tions of the two materials will be different, which means that additional conditions of compatibility would be necessary. The same happens in the case of a temperature variation, if the coefficients of thermal expansion of the two materials are different. However, it can be shown that these stresses are sufficiently small to be ignored, which allows the use of the constitutive law in this one-dimensional form. Section VII.6 gives an analysis of the error introduced by this approximation in the case of axial force and bending.

area of material b by the homogenizing coefficient of material b in material a , m_a .

The elongation of a bar of length l may be computed from the stress in any material, since the strain is constant, yielding

$$\varepsilon = \frac{\sigma_a}{E_a} = \frac{\sigma_b}{E_b} \Rightarrow \Delta l = \varepsilon l = \frac{\sigma_a}{E_a} l = \frac{\sigma_b}{E_b} l = \frac{Nl}{E_a\Omega_a + E_b\Omega_b}. \quad (134)$$

VI.6.d Effects of Temperature Variations

As shown in Sect. VI.6.a, a temperature variation introduces stresses in a prismatic bar made of two materials with different thermal expansion coefficients. Generally, even a uniform temperature variation causes bending, i.e., the axis of the bar does not remain a straight line, as in the example given in Fig. 65 (α_a and α_b are the coefficients of thermal expansion of materials a and b).

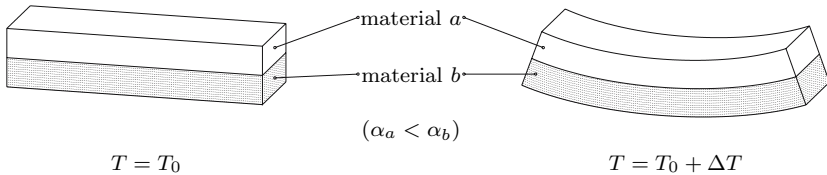


Fig. 65. Effect of a uniform temperature variation on a composite bar

The study of the stresses generated by that bending requires the bending theory which is explained in Chap. VII. However, if the cross section has two symmetry axes, i.e., if the prismatic bar has two longitudinal symmetry planes, its axis must remain a straight line, which means that the deformation is purely axial.³

In order to analyse the internal forces in the connection between the two materials, let us analyse the whole bar and not just a cross-section. The symmetry principle (Fig. 58) only permits the conclusion that the middle section of the bar remains plane in the deformation. Thus, the strain is constant in this section, which allows the computation of the stresses in the two materials, using the same equilibrium and compatibility conditions as in the case of the axial force, yielding

$$\begin{cases} \varepsilon = \frac{\sigma_a}{E_a} + \alpha_a \Delta T = \frac{\sigma_b}{E_b} + \alpha_b \Delta T \\ N = \sigma_a \Omega_a + \sigma_b \Omega_b = 0 \end{cases} \Rightarrow \begin{cases} \sigma_a = \frac{E_a E_b \Omega_a \Omega_b}{E_a \Omega_a + E_b \Omega_b} \Delta T \frac{\alpha_b - \alpha_a}{\Omega_a} \\ \sigma_b = \frac{E_a E_b \Omega_a \Omega_b}{E_a \Omega_a + E_b \Omega_b} \Delta T \frac{\alpha_a - \alpha_b}{\Omega_b} \end{cases}. \quad (135)$$

³The double symmetry of the cross-section is a sufficient condition for purely axial deformation. This condition may, however, not be necessary (see examples VI.20 and VI.21).

If an axial force is also acting, the total stresses may be computed by adding the stresses given by (133) and (135), since the superposition principle may be applied in the case of temperature variation (cf. Sect. V.8).

The cross-sections located near by the ends of the bar can not remain plane. In fact, if the end cross-sections remain plain, the stresses given by (135) act on them. This is not possible, since no external forces are applied. In order to clarify this issue, let us consider a rigid block connected to each end of the bar, as represented in Fig. 66-a. In this case, all cross-sections remain plain and (135) is valid for the whole bar.⁴

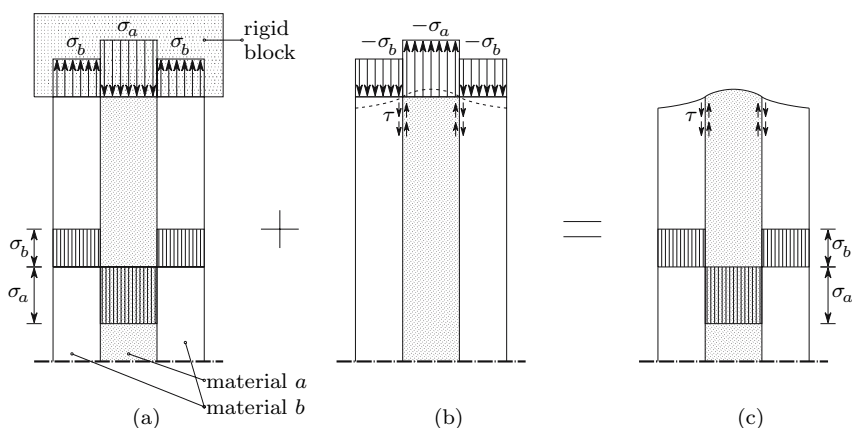


Fig. 66. Transmission of internal forces between the two materials in a composite member under a uniform temperature variation ($\Delta T > 0$ and $\alpha_a > \alpha_b$ or $\Delta T < 0$ and $\alpha_a < \alpha_b$)

The real stress distribution in the bar may be obtained by the superposition principle. To this end, let us superpose upon the situation corresponding to Fig. 66-a the loading situation illustrated in Fig. 66-b, where no temperature variation takes place and only end distributed loads act, corresponding to the stress distribution given by (135) with reversed direction. These stresses have a vanishing resultant ($N = 0$, cf. (135)). Thus, the Saint-Venant's principle leads to the conclusion that its effect is restricted to the region of the bar around its ends. The stress distribution in this region depends on the shape of the cross-section and cannot be obtained by means of the theory of slender members. However, a qualitative analysis of Fig. 66-b leads to the conclusion that shearing stresses τ must appear in the interface between the two materials. By superposing the stresses corresponding to the loading situa-

⁴This conclusion is easily arrived at by symmetry considerations: considering the part of the bar defined by the end and the central cross sections, we conclude that the middle section of this piece (the quarter length cross-section) remains plane. Further sub-division leads to the conclusion that every section must remain plane.

tions represented in Figs. 66-a and 66-b, we may conclude that these shearing stresses transmit the internal forces from one material to the other (Fig. 66-c). This analysis allows the conclusion that, irrespective of the member's length, these shearing stresses appear only near by the ends of the bar. Furthermore, they do not depend on the length of the bar.

VI.7 Non-Prismatic Members

VI.7.a Introduction

In the development of the expressions presented in the previous sections for the stresses in members under axial loading, only prismatic bars were considered, since the symmetry conditions leading to the law of conservation of plane sections are only valid for this special kind of slender members. However, these expressions are generally used for non-prismatic members, i.e. bars with a curved axis or with a non-constant cross-section. This leads to errors, since those expressions are only exact for prismatic bars. The magnitude of these errors depends on the relation between the curvature radius and the cross-section's dimension in the direction of that radius, in the case of curved members, and on the rate of variation of the cross-section's dimensions, in the case of a non-constant cross-section. In order to get an idea of the importance of these errors, we can compare approximate solutions obtained by means of the theory of prismatic bars with the exact results furnished by the Theory of Elasticity in particular cases.

VI.7.b Slender Members with Curved Axis

As an example of a slender member with a curved axis, we may take a ring defined by a slice of length b of a tube with constant wall thickness under an internal pressure p . The tube's dimensions are defined by the thickness e and the mean radius r_m , as shown in Fig. 67.

The mean stress acting on the tube's wall σ_{med} may be obtained by equilibrium considerations on a half ring (Fig. 67)

$$p2\left(r_m - \frac{e}{2}\right)b = 2\sigma_{\text{med}}eb \Rightarrow \left| \begin{array}{l} \sigma_{\text{med}} = \frac{p\left(r_m - \frac{e}{2}\right)}{e} = p\left(\frac{1}{\alpha} - \frac{1}{2}\right) \\ \text{with } \alpha = \frac{e}{r_m} \end{array} \right. \quad (136)$$

This stress coincides with the solution obtained by considering the ring as a slender member, since, according to the theory of prismatic members, the stress is constant in the cross-section.

This problem is solved by Theory of Elasticity (Lamé's problem [4]) using polar coordinates. The solution is described by radial and circumferential stresses. The latter coincide with the stresses in the cross-section of the ring.

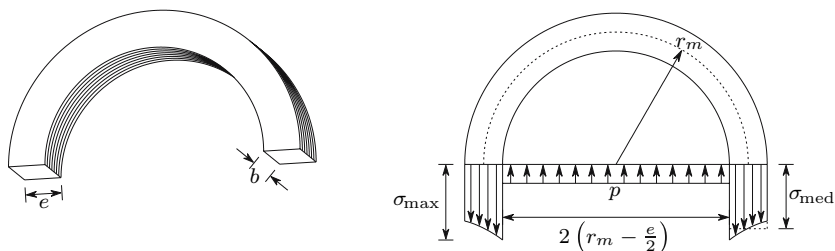


Fig. 67. Forces acting on a tube under internal pressure

The maximum circumferential stress occurs at the inner surface of the tube (σ_{\max} , Fig. 67), taking the value

$$\sigma_{\max} = \frac{p}{\alpha} \left(1 + \frac{\alpha^2}{4} \right).$$

The relation between the maximum and mean stress (136) is given by

$$\frac{\sigma_{\max}}{\sigma_{\text{med}}} = \frac{1 + \frac{\alpha^2}{4}}{1 - \frac{\alpha}{2}}.$$

The following table gives the error of the approximate solution furnished by the theory of prismatic members, as a function of parameter α .⁵

$\alpha = e/r_m$	0.01	0.02	0.05	0.1	0.2
$\sigma_{\max}/\sigma_{\text{med}}$	1.0051	1.0102	1.0263	1.0553	1.1222
Error	0.51%	1.02%	2.63%	5.53%	12.22%

If the value of 5% is accepted as the maximum admissible error, we conclude, generalizing to other cases of curved bars under axial force, that the theory of prismatic bars does not introduce a significant error, while the dimension of the cross-section in the curvature plane is less than 0.1 times the dimension of the mean radius of the member.

The cross-sections of the ring still remain plane, although the bar is not prismatic, since the plane containing any cross-section of the ring is a symmetry plane. The inner pressure causes a diameter increase in the tube. If

⁵Equation (136), although similar, is not the same as the well known formula for the computation of the mean stress in a thin-walled tube under internal pressure $\sigma_{\text{med}} = pr_m/e$. This expression is obtained in the same way as (136), with the difference that the mean radius r_m is used in place of the inner radius $r_m - e/2$. If this expression is used instead of (136), the error on the computation of the maximum stress will be significantly lower. For example, for $\alpha = 0.2$ an error of about 1% is obtained. This expression was not used here, however, since the purpose of the analysis is to investigate the error introduced by the use of the theory of prismatic bars in curved members and not to compute the stresses in tubes.

the deformation caused by the radial stresses is ignored, the elongation at the inner and outer sides of the wall is equal. However, as the undeformed distance between two cross-sections is smaller at the inner side, the strain and, consequently, the stress is larger there.

VI.7.c Slender Members with Variable Cross-Section

As a simple example of a member with variable cross-section, with an exact solution furnished by the Theory of Elasticity, the wedge shaped element represented in Fig. 68 is considered.

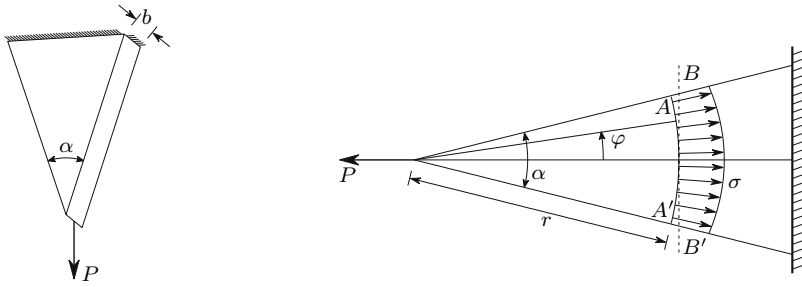


Fig. 68. Stresses in a slender member with variable cross-section

The solution of Theory of Elasticity is obtained for this problem by means of polar coordinates [4] and indicates that in a cylindrical section (AA' , Fig. 68) the tangential (shearing) stress vanishes and the radial stress σ is given by the expression below (r and φ are the polar coordinates)

$$\sigma = \frac{2}{\alpha + \sin \alpha} \frac{P \cos \varphi}{br}.$$

For a given value of r , this normal stress reaches its maximum for $\varphi = 0$, taking the value

$$\varphi = 0 \Rightarrow \sigma = \sigma_{\max} = \frac{2}{\alpha + \sin \alpha} \frac{P}{br}.$$

The theory of prismatic bars yields for the stress in the cross-section BB' the value

$$\sigma_{\text{med}} = \frac{P}{\Omega} = \frac{P}{2br \tan \frac{\alpha}{2}}.$$

The error affecting the last solution may be expressed by the relation between σ_{\max} and σ_{med}

$$\frac{\sigma_{\max}}{\sigma_{\text{med}}} = \frac{4 \tan \frac{\alpha}{2}}{\alpha + \sin \alpha}.$$

This relation depends only on angle α and takes the values

α	10°	20°	30°	45°	60°
$\sigma_{\max}/\sigma_{\text{med}}$	1.0051	1.0206	1.0471	1.1101	1.2071
Error	0.51%	2.06%	4.71%	11.01%	20.71%

We conclude that for small values of angle α , which expresses in this case the rate of variation of the cross-section's dimensions, the error is very small.

VI.8 Non-Constant Axial Force – Self-Weight

The symmetry considerations used to demonstrate the law of conservation of plane sections are not satisfied in the case of a non-constant axial force, caused, for example, by the self-weight in non-horizontal bars, which means that there is no guarantee that the cross-sections remain plane. Furthermore, experimental observation shows that in the deformation caused by self-weight the sections do not remain plane (Fig. 69).

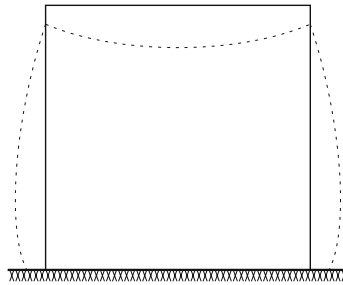


Fig. 69. Deformation of a prism of jelly under its self-weight

However, the solution of the Theory of Elasticity for a vertical homogeneous prism under its self-weight, shows that the stress is constant in the cross-section, although it does not remain plane (see example VI.12).⁶ Although the generalization of this solution to other cases is not straightforward, it shows that a uniform distribution of the stress in the cross-section is possible, even without the conservation of plane sections. Besides, the self-weight of axially loaded structural members usually causes only a very small fraction of the total axial force, so that only a very small loss of symmetry occurs in the forces acting in a piece of the prismatic bar. For these reasons, the elongation Δl of a bar with length l , caused by a variable axial force $N(z)$, may be computed by the expression

⁶The law of conservation of plane sections is a sufficient condition to have a constant stress in the cross-section of a bar under purely axial force. This condition may, however, not be necessary, as the solution referred to shows.

$$d\Delta l = \frac{N}{E\Omega} dz \Rightarrow \Delta l = \frac{1}{E} \int_0^l \frac{N}{\Omega} dz, \quad (137)$$

where z is a coordinate with the direction of the bar's axis. This expression is also valid in the case of a non-constant cross-section, provided that the rate of variation is small, as seen in Sect. VI.7.

VI.9 Stress Concentrations

In the neighbourhood of discontinuities in the bar, such as holes, notches, sudden changes of the cross-section, etc., the theory of prismatic bars is no longer valid, the cross-sections do not remain plane and the stress distribution is not uniform, which means that the maximum stress is larger than the mean value furnished by the theory of prismatic members. In the example depicted in Fig. 70 of a bar of constant thickness with two small semi-circular cuts ($r \ll b$), the maximum stress in the cross-section which contains the centers of the cuts is approximately twice the mean stress. We have in this case a *stress concentration factor* of 2.

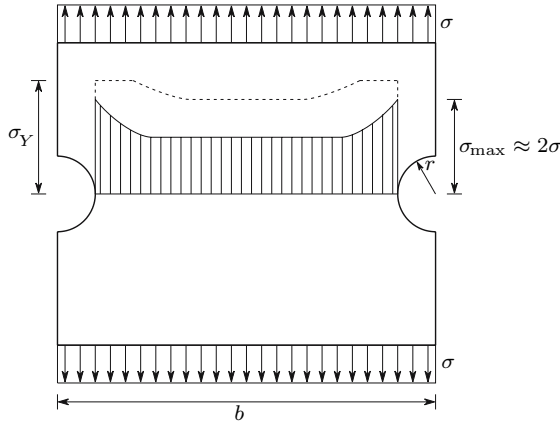


Fig. 70. Example of stress concentration caused by two semi-circular cuts ($r \ll b$). ---- redistribution of stresses in the case of a ductile material by plastic deformation

The consideration of the stress concentrations in the safety evaluation is especially important in the case of brittle materials, since in this case there is no possibility of stress redistribution. The rupture process is similar to the one described in Sect. V.6: a crack starts at the points of stress concentration and propagates immediately to the rest of the cross-section, since the stress concentration at the tip of the crack is even larger, as will be seen later.

In the case of a ductile material, stress redistribution takes place, since the zones where the yielding strain is attained at first retain the loading capacity

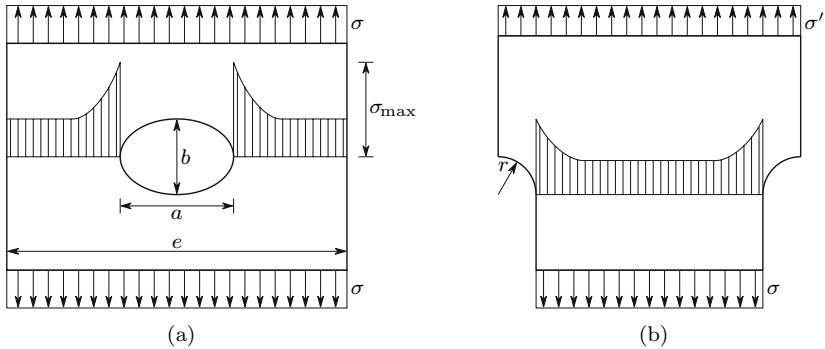


Fig. 71. Examples of stress concentration

described by the yielding stress σ_Y , until the whole cross-section yields, as indicated by the dashed line in Fig. 70. This is why the stress concentration is often not considered in the case of ductile materials. However, if the member is under cyclically varying loads, the stress concentration must be taken into account, due to the risk of fatigue failure, as seen in Sect. V.6.

In Fig. 71 two other examples of stress concentration are presented. In the first one (Fig. 71-a) a bar with a rectangular cross-section and a small thickness has an elliptical hole, with one of the ellipse's principal axes coinciding with the axis of the bar. The Theory of Elasticity furnishes a solution for the stress distribution in this case. The maximum stress takes the value [4]

$$\sigma_{\max} = \left(1 + 2\frac{a}{b}\right) \sigma ,$$

provided that the transversal dimension of the hole is very small, as compared with the width of the bar ($a \ll e$). From this expression we conclude that for $a = b$ (circular hole) the stress concentration factor is 3 ($\sigma_{\max} = 3\sigma$). The stress concentration increases if the larger axis has the transversal direction ($a > b$) and decreases in the opposite case. In particular, for $a = 0$ (a crack parallel to the axis of the bar) there will be no stress concentration. In the opposite case $b = 0$ (perpendicular crack in relation to axial force) we have an infinite stress concentration factor: $\sigma_{\max} = \infty$!!! Obviously this value is a purely theoretical one, since it is computed by considering that the material is perfectly continuous and has a linear elastic behaviour. However, the continuity hypothesis ceases to be acceptable when b takes a value similar to the dimension of the metal crystals or other material particles. Besides, the material does not retain linear elastic behaviour for large stress. It can be proved that a very small plastic deformation substantially reduces the stress concentration. Nevertheless, this example illustrates the danger of a transversal crack to the safety of a structure, in the case of brittle material, or cyclic loads (fatigue failure).

In Fig. 71-b an example of a suddenly changing cross-section is presented, where the transition is made by means of circular fillets. The stress concentration increases as the difference between the two cross-sections increases and as the radius of the fillet decreases.

VI.10 Examples and Exercises

VI.1. The truss described in Fig. VI.1-a is made of a material with linear elastic behaviour with a modulus of elasticity E .

- Considering a nominal strength σ_{all} and knowing that buckling is prevented, determine the minimum cross-section area of bars \overline{AB} and \overline{BC} .
- Considering these cross-section areas compute the displacement of point B .

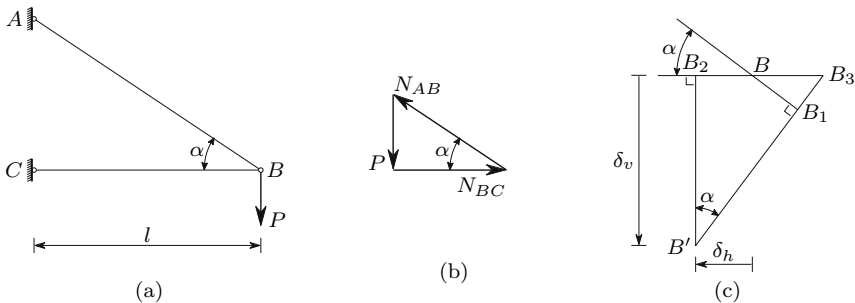


Fig. VI.1

Resolution

- The axial forces in the bars may be computed by means of the vertical and horizontal equilibrium conditions of the forces acting in node B (Fig. VI.1-b), yielding

$$N_{AB} = \frac{P}{\sin \alpha} \quad N_{BC} = \frac{P}{\tan \alpha} \quad (\text{compression}).$$

Equation (115) gives the minimum areas of the cross-sections

$$\Omega_{AB} = \frac{N_{AB}}{\sigma_{\text{all}}} = \frac{P}{\sigma_{\text{all}} \sin \alpha} \quad \text{and} \quad \Omega_{BC} = \frac{N_{BC}}{\sigma_{\text{all}}} = \frac{P}{\sigma_{\text{all}} \tan \alpha}.$$

- The displacement of point B is caused by the changes in the length of the two bars. The corresponding values may be computed by means of (116), yielding

$$\Delta l_{AB} = \frac{N_{AB} l_{AB}}{E \Omega_{AB}} = \frac{\frac{P}{\sin \alpha} \frac{l}{\cos \alpha}}{E \frac{P}{\sigma_{\text{all}} \sin \alpha}} = \frac{l \sigma_{\text{all}}}{E \cos \alpha}$$

and

$$\Delta l_{BC} = \frac{N_{BC} l_{BC}}{E \Omega_{BC}} = \frac{\frac{P}{\tan \alpha} l}{E \frac{P}{\sigma_{\text{all}} \tan \alpha}} = \frac{l \sigma_{\text{all}}}{E}.$$

As a consequence of the bars' variations in length, the position of point B changes to the intersection of the two circumference arcs, whose centers are points A and C and whose radii are the lengths of the deformed bars. Since the deformations are very small, as compared with the truss' dimensions, the rotation of the bars will also be very small, which allows the substitution of the circumference arcs by straight lines, as shown in the graphic construction presented in Fig. VI.1-c. In this Figure the elongation of bar \overline{AB} is represented by the line segment $\overline{BB_1}$, the length reduction of bar \overline{BC} is $\overline{BB_2}$ and the circumference axes are approximated by the line segments $\overline{B_1B'}$ and $\overline{B_2B'}$. The intersection of these segments (point B') defines the position of point B after the deformation.

The horizontal component of the displacement is then

$$\delta_h = \overline{BB_2} = \Delta l_{BC} = \frac{l \sigma_{\text{all}}}{E}.$$

The vertical component may be computed by means of the auxiliary distance $\overline{BB_3} = \frac{\overline{BB_1}}{\cos \alpha} = \frac{\Delta l_{AB}}{\cos \alpha}$, yielding

$$\delta_v = \overline{B_2B'} = \frac{\overline{B_2B_3}}{\tan \alpha} = \frac{\Delta l_{BC} + \frac{\Delta l_{AB}}{\cos \alpha}}{\tan \alpha} = \frac{l \sigma_{\text{all}}}{E} \left(\frac{1}{\tan \alpha} + \frac{1}{\sin \alpha \cos \alpha} \right).$$

VI.2. The truss represented in Fig. VI.2-a is made of a material with an elasticity modulus E and a thermal expansion coefficient α . Determine the expressions required to compute the displacement of point B , caused by the force P and by a temperature increase ΔT .

Resolution

The axial forces in the bars may be computed by means of the equilibrium conditions of the forces acting in node B , which are represented by the system of equations (Fig. VI.2-b)

$$\begin{cases} N_1 \cos \alpha_1 = N_2 \cos \alpha_2 \\ N_1 \sin \alpha_1 + N_2 \sin \alpha_2 = P. \end{cases}$$

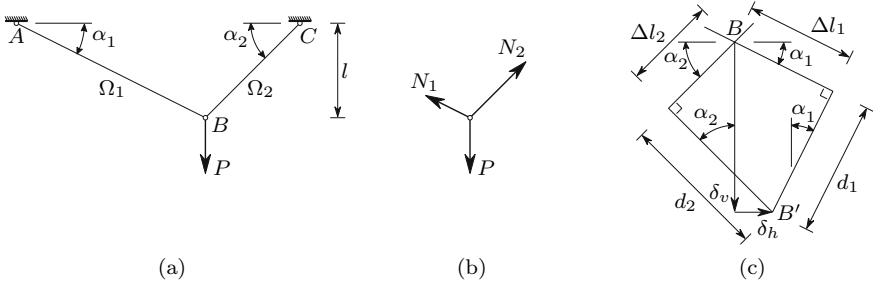


Fig. VI.2

The deformation of the bars under the axial forces and the temperature variation may be computed by means of (117), yielding

$$\Delta l_1 = \left(\frac{N_1}{E\Omega_1} + \alpha\Delta T \right) \frac{l}{\sin \alpha_1} \quad \text{and} \quad \Delta l_2 = \left(\frac{N_2}{E\Omega_2} + \alpha\Delta T \right) \frac{l}{\sin \alpha_2} .$$

The horizontal and vertical components of the displacement of point B (δ_h and δ_v) may be computed by means of the graphical construction presented in Fig. VI.2-c. From this Figure the following relations may be established.

$$\begin{aligned} \delta_v &= d_1 \cos \alpha_1 + \Delta l_1 \sin \alpha_1 = d_2 \cos \alpha_2 + \Delta l_2 \sin \alpha_2 \\ \delta_h &= \Delta l_1 \cos \alpha_1 - d_1 \sin \alpha_1 = d_2 \sin \alpha_2 - \Delta l_2 \cos \alpha_2 . \end{aligned}$$

By solving the system formed by the second equalities of each one of these expressions the distances d_1 and d_2 may be obtained. After this, δ_v and δ_h are immediately obtained. As an alternative, the projections of δ_v and δ_h on the directions of Δl_1 and Δl_2 yield the following system of equations

$$\begin{cases} \delta_v \sin \alpha_1 + \delta_h \cos \alpha_1 = \Delta l_1 \\ \delta_v \sin \alpha_2 - \delta_h \cos \alpha_2 = \Delta l_2 , \end{cases}$$

whose solution directly gives δ_v and δ_h .

VI.3. Consider a bar of cross-section area Ω , with built-in supports in both ends, made of a material with an elasticity modulus E and a thermal expansion coefficient α . Using the force and the displacement methods, compute the axial force introduced into the bar by a uniform temperature reduction ΔT , in relation to the construction temperature.

Resolution

Force method

Since it is known that all internal forces, except the axial force, vanish, the degree of static indeterminacy is one, although the bar has twelve external

connections (six at each end) and only six are necessary to guarantee the static equilibrium.

If we suppose that one of the supports of the bar is removed, it becomes statically determined and, as a consequence, the temperature variation does not cause internal forces, but only a length reduction with the value

$$\Delta l = \alpha \Delta T l ,$$

where l represents the bar's length. The axial force in the bar with the two supports is the force needed to prevent the length reduction. In other words, it is the force which causes an elongation with the same value as the length reduction caused by the temperature variation. Using (116) and this condition, we get

$$\alpha \Delta T l = \frac{Nl}{E\Omega} \Rightarrow N = E\Omega\alpha\Delta T .$$

Displacement Method

The degree of kinematic indeterminacy of this structure is zero, since the displacement of any cross-section is zero. We easily reach this conclusion by symmetry considerations: the middle cross-section has zero displacement; taking half the bar, we conclude that its middle section (the quarter length section) does not move, and so on. As a consequence, the total strain caused by the axial force and by the temperature variation is also zero. From (117) we get, since the temperature variation is negative ($\Delta T < 0$)

$$\varepsilon = \frac{\Delta l}{l} = \frac{N}{E\Omega} - \alpha\Delta T = 0 \Rightarrow N = E\Omega\alpha\Delta T .$$

VI.4. Consider the bar represented in Fig. VI.4, which is made of a material with elasticity modulus E and thermal expansion coefficient α and has three zones with different cross-section areas. Using the force and the displacement methods, compute the axial force introduced into the bar by a uniform temperature reduction ΔT , in relation to the construction temperature.

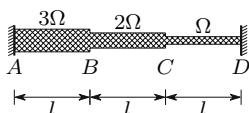


Fig. VI.4

*Resolution**Force Method*

Using the same reasoning as in example VI.3, we conclude immediately that the degree of static indeterminacy is one. The axial force may be computed in the same way. The length reduction caused by the temperature variation takes the value

$$\Delta l = 3\alpha\Delta Tl .$$

The elongation caused by the axial force is the sum of the elongations in the three zones. Since this elongation must compensate for the length reduction Δl , we have

$$\left\{ \begin{array}{l} \Delta l_{AB} = \frac{Nl}{3E\Omega} \\ \Delta l_{BC} = \frac{Nl}{2E\Omega} \\ \Delta l_{CD} = \frac{Nl}{E\Omega} \end{array} \right. \Rightarrow 3\alpha\Delta Tl = \frac{Nl}{E\Omega} \left(\frac{1}{3} + \frac{1}{2} + 1 \right) \Rightarrow N = \frac{18}{11}E\Omega\alpha\Delta T .$$

Displacement Method

Resolving this problem by means of the displacement method is a little more lengthy than by using the force method, since the degree of kinematic indeterminacy is two. In fact, if the displacements of points B and C are known, the strains and stresses in each zone may be immediately computed. Denoting by δ_1 and δ_2 the displacements of sections B and C , respectively, considered as positive from left to right, we get from (117), taking into consideration that the axial force N is the same in the whole bar

$$\begin{aligned} \Delta l_{AB} = \delta_1 &= \frac{Nl}{3E\Omega} - \alpha\Delta Tl &\Rightarrow N &= \frac{E\Omega}{l} (3\delta_1 + 3\alpha\Delta Tl) \\ \Delta l_{BC} = \delta_2 - \delta_1 &= \frac{Nl}{2E\Omega} - \alpha\Delta Tl &\Rightarrow N &= \frac{E\Omega}{l} [2(\delta_2 - \delta_1) + 2\alpha\Delta Tl] \\ \Delta l_{CD} = -\delta_2 &= \frac{Nl}{E\Omega} - \alpha\Delta Tl &\Rightarrow N &= \frac{E\Omega}{l} (-\delta_2 + \alpha\Delta Tl) . \end{aligned}$$

By eliminating N from these equations we get a system of two equations, which allows the computation of δ_1 and δ_2 , yielding

$$\left\{ \begin{array}{l} 3\delta_1 + 3\alpha\Delta Tl = 2(\delta_2 - \delta_1) + 2\alpha\Delta Tl \\ 3\delta_1 + 3\alpha\Delta Tl = -\delta_2 + \alpha\Delta Tl \end{array} \right. \Rightarrow \left\{ \begin{array}{l} \delta_1 = -\frac{5}{11}\alpha\Delta Tl \\ \delta_2 = -\frac{7}{11}\alpha\Delta Tl . \end{array} \right.$$

Any of the three relations between the axial force N and the displacements δ_1 and δ_2 allows the computation of N . Using the first, for example, we get

$$N = \frac{3E\Omega}{l} (\delta_1 + \alpha\Delta Tl) = \frac{3E\Omega}{l} \left(-\frac{5}{11} + 1 \right) \alpha\Delta Tl = \frac{18}{11}E\Omega\alpha\Delta T .$$

VI.5. The bar represented in Fig. VI.5 is made of a material with an elasticity modulus E and a thermal expansion coefficient α . The bar has a rectangular cross-section with a constant thickness a . Determine the axial force caused by a uniform temperature reduction ΔT .

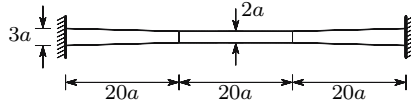


Fig. VI.5

Resolution

The resolution of this problem by the displacement method requires the prior computation of the relation between the axial force and the elongation in a bar with variable cross-section. The problem is, however, easily solved by the force method. The statically determinate base structure may be obtained by removing the right support, for example. In this situation the temperature variation causes the length reduction

$$\Delta l_T = \alpha l \Delta T = \alpha 60a \Delta T .$$

The axial force N must cause an elongation which compensates for this length reduction. Considering a coordinate z with its origin on the left support, with increasing values from left to right, we may express the cross-section area as a function of z . For values of z between 0 and $20a$ we get

$$\Omega(z) = 3a^2 - \frac{a}{20} z .$$

As the middle section of the bar is in a symmetry plane, the total elongation caused by the axial force N is given by

$$\begin{aligned} \Delta l_N &= \int_0^l \frac{N}{E\Omega} dz = 2 \int_0^{20a} \frac{N}{E(3a^2 - \frac{a}{20}z)} dz + \int_0^{20a} \frac{N}{2Ea^2} dz \\ &= 2 \frac{N}{E} \left[-\frac{20}{a} \ln \left(3a^2 - \frac{a}{20}z \right) \right]_0^{20a} + \frac{10N}{Ea} = \left[40 \ln \left(\frac{3}{2} \right) + 10 \right] \frac{N}{Ea} . \end{aligned}$$

The equality $\Delta l_T = \Delta l_N$ describes the condition of deformation compatibility. The solution of this equation yields the value of the axial force

$$\Delta l_T = \Delta l_N \Rightarrow N = \frac{60\alpha E \Delta T a^2}{40 \ln \left(\frac{3}{2} \right) + 10} \approx 2.28845 \alpha E \Delta T a^2 .$$

VI.6. The bar \overline{AB} of the structure represented in Fig. VI.6-a has a sufficiently high stiffness to be considered as rigid. The three suspension cables

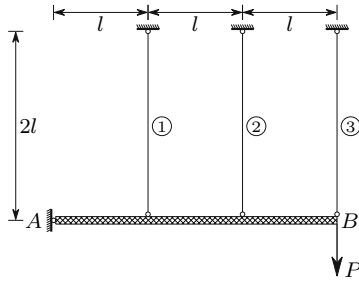


Fig. VI.6-a

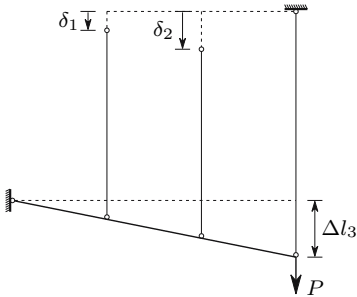


Fig. VI.6-b

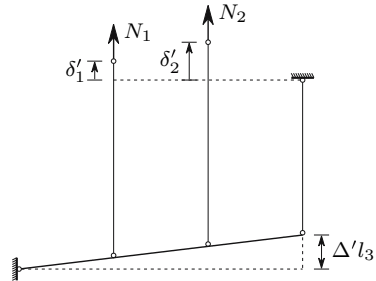


Fig. VI.6-c

have the same cross-section area Ω and are made of a material with an elasticity modulus E .

Compute the axial forces in the cables using:

- (a) the force method;
- (b) the displacement method.

Resolution

- (a) The structure has a degree of static indeterminacy of two. Thus, the statically determinate base structure is obtained by releasing two connections. In this case, the vertical connections on the top of bars 1 and 2 are released (Fig. VI.6-b). Under these conditions the axial force in bar 3 takes the value P . The corresponding elongation and the displacements of the top ends of bars 1 and 2 are

$$N_3 = P \Rightarrow \Delta l_3 = \frac{P2l}{E\Omega} \Rightarrow \begin{cases} \delta_1 = \frac{1}{3}\Delta l_3 = \frac{2}{3}\frac{Pl}{E\Omega} \\ \delta_2 = \frac{2}{3}\Delta l_3 = \frac{4}{3}\frac{Pl}{E\Omega} \end{cases}.$$

The displacements caused by axial forces in bars 1 and 2, N_1 and N_2 , in the released connections of the statically determinate base structure, δ'_1 and δ'_2 (Fig. VI.6-c), must compensate for the displacements δ_1 and δ_2 caused

by force P . The axial compressive force in bar 3 and the corresponding length reduction $\Delta'l_3$ (Fig. VI.6-c) take the values

$$N'_3 = \frac{1}{3}N_1 + \frac{2}{3}N_2 \qquad \Delta'l_3 = \frac{N'_3 2l}{E\Omega} = \frac{2}{3} \frac{l}{E\Omega} (N_1 + 2N_2) .$$

The displacements δ'_1 and δ'_2 are caused by the rotation of the rigid bar \overline{AB} and by the elongations in bars 1 and 2, respectively

$$\begin{aligned} \delta'_1 &= \frac{1}{3}\Delta'l_3 + \frac{N_1 2l}{E\Omega} = \frac{l}{E\Omega} \left(\frac{20}{9}N_1 + \frac{4}{9}N_2 \right) \\ \delta'_2 &= \frac{2}{3}\Delta'l_3 + \frac{N_2 2l}{E\Omega} = \frac{l}{E\Omega} \left(\frac{4}{9}N_1 + \frac{26}{9}N_2 \right) . \end{aligned}$$

The conditions of compatibility of the deformations in the released connections define a system of two equations, whose solution gives the values of N_1 and N_2

$$\begin{cases} \delta_1 = \delta'_1 \\ \delta_2 = \delta'_2 \end{cases} \Rightarrow \begin{cases} \frac{2}{3} \frac{Pl}{E\Omega} = \frac{l}{E\Omega} \left(\frac{20}{9}N_1 + \frac{4}{9}N_2 \right) \\ \frac{4}{3} \frac{Pl}{E\Omega} = \frac{l}{E\Omega} \left(\frac{4}{9}N_1 + \frac{26}{9}N_2 \right) \end{cases} \Rightarrow \begin{cases} N_1 = \frac{3}{14}P \\ N_2 = \frac{6}{14}P . \end{cases}$$

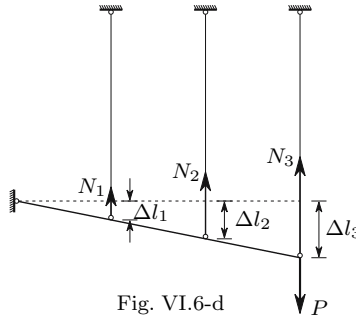
The axial force in bar 3 may now be obtained by equilibrium considerations. The condition of equilibrium of moments in relation to point A gives

$$N_1 l + N_2 2l + N_3 3l = P 3l \Rightarrow N_3 = P - \frac{1}{3}N_1 - \frac{2}{3}N_2 = \frac{9}{14}P .$$

- (b) The solution of the problem by means of the displacement method is substantially easier, since the degree of kinematic indeterminacy is one. In fact, once the rotation of the rigid bar \overline{AB} is known, the elongation of the bars is defined, which allows the immediate computation of the axial forces. Taking as kinematic parameter the displacement $\delta = \Delta'l_3$ of point B (Fig. VI.6-d), we get the following values for the axial forces in the three bars

$$\begin{aligned} \Delta l_1 &= \frac{N_1 2l}{E\Omega} = \frac{1}{3}\delta \Rightarrow N_1 = \frac{E\Omega}{6l}\delta ; \\ \Delta l_2 &= \frac{N_2 2l}{E\Omega} = \frac{2}{3}\delta \Rightarrow N_2 = \frac{E\Omega}{3l}\delta ; \\ \Delta l_3 &= \frac{N_3 2l}{E\Omega} = \delta \Rightarrow N_3 = \frac{E\Omega}{2l}\delta . \end{aligned}$$

The condition of equilibrium of moments in relation to point A furnishes a relation between P and δ , yielding



$$P3l = N_1l + N_22l + N_33l = \left(\frac{1}{6} + \frac{2}{3} + \frac{3}{2} \right) E\Omega\delta \Rightarrow \delta = \frac{18}{14} \frac{Pl}{E\Omega}.$$

Substitution of this value in the relations above, yields the same values of N_1 , N_2 and N_3 , as obtained by the force method.

- VI.7. In the structure represented in Fig. VI.7-a the bar \overline{AB} may be considered as rigid. The suspension bars are made of an elastic, perfectly plastic material with a modulus of elasticity E and a yielding stress σ_Y .
- Determine the sequence of yielding of the bars, when the load P varies from zero to the value which causes the collapse of the structure.
 - Compute the value of P which causes the yielding of the structure and the displacement of point C just before the collapse.
 - Compute the values of the loads and displacements corresponding to the yielding of the remaining bars.

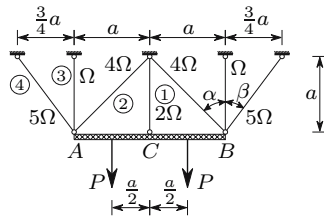


Fig. VI.7-a

Resolution

- The degree of kinematic indeterminacy is one, since the symmetry of the structure leads to the conclusion that both the horizontal displacement and the rotation of bar \overline{AB} are zero. Choosing as kinematic parameter

the vertical displacement δ of the rigid bar, we may express the strains in the bars as functions of δ , obtaining (Fig. VI.7-b)

$$\begin{cases} \Delta l_1 = \Delta l_3 = \delta \\ l_1 = l_3 = a \end{cases} ; \Delta l_1 = \varepsilon_1 a = \delta \Rightarrow \varepsilon_1 = \varepsilon_3 = \frac{\delta}{a}$$

$$\begin{cases} \Delta l_2 = \delta \cos \alpha \\ l_2 = \frac{a}{\cos \alpha} \end{cases} ; \Delta l_2 = \varepsilon_2 l_2 = \varepsilon_2 \frac{a}{\cos \alpha} = \delta \cos \alpha \Rightarrow \varepsilon_2 = \frac{1}{a} \cos^2 \alpha \delta = 0.5 \frac{\delta}{a}$$

$$\begin{cases} \Delta l_4 = \delta \cos \beta \\ l_4 = \frac{a}{\cos \beta} \end{cases} ; \Delta l_4 = \varepsilon_4 l_4 = \varepsilon_4 \frac{a}{\cos \beta} = \delta \cos \beta \Rightarrow \varepsilon_4 = \frac{1}{a} \cos^2 \beta \delta = 0.64 \frac{\delta}{a} .$$

Since we have $\varepsilon_1 = \varepsilon_3 > \varepsilon_4 > \varepsilon_2$, we conclude that bars 1 and 3 yield at first and are followed by bars 4. Bars 2 yield last, leading to the collapse of the structure.

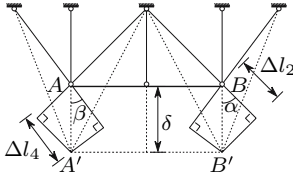


Fig. VI.7-b

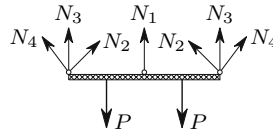


Fig. VI.7-c

- (b) The structural collapse occurs when all suspension bars yield. At this moment the stresses in all bars take the value of the yielding stress σ_Y . The corresponding value of P may be computed by means of the condition of vertical equilibrium of the forces acting on the rigid bar \overline{AB} (Fig. VI.7-c), yielding

$$\begin{aligned} P &= \frac{N_1}{2} + N_2 \cos \alpha + N_3 + N_4 \cos \beta \\ &= \Omega \sigma_Y + 4\Omega \sigma_Y \cos \alpha + \Omega \sigma_Y + 5\Omega \sigma_Y \cos \beta = 8.8284\Omega \sigma_Y . \end{aligned}$$

As bars 2 yield last, the displacement of point C just before the collapse is the value of δ corresponding to $\varepsilon_2 = \varepsilon_Y$. Thus, we have

$$\varepsilon_2 = \frac{\sigma_Y}{E} = \frac{1}{2a} \delta_Y \Rightarrow \delta_Y = 2 \frac{a \sigma_Y}{E} .$$

- (c) When bars 1 and 3 start yielding, the kinematic parameter δ takes the value corresponding to the yielding strain in these bars, which is $\delta = a \varepsilon_Y = \frac{a \sigma_Y}{E}$. The axial forces in the remaining bars may be obtained from the relations between the strains and the displacement δ . The corresponding value of P is then obtained by means of the vertical equilibrium

condition. This computation sequence is summarized by the following expressions

$$\delta = a \frac{\sigma_Y}{E} \Rightarrow \begin{cases} N_1 = 2\Omega\sigma_Y \\ N_2 = 4\Omega E \varepsilon_2 = 4\Omega E \frac{1}{a} \cos^2 \alpha \delta = 2\Omega\sigma_Y \\ N_3 = \Omega\sigma_Y \\ N_4 = 5\Omega E \varepsilon_4 = 5\Omega E \frac{1}{a} \cos^2 \beta \delta = 3.2\Omega\sigma_Y \end{cases} \Rightarrow P = 5.9742\Omega\sigma_Y .$$

Yielding of bars 4 takes place for $\delta = \frac{a\varepsilon_Y}{\cos^2 \beta} = 1.5625 \frac{a\sigma_Y}{E}$. At this stage bars 1 and 3 are already over the yielding strain. Only bars 2 are still in the elastic range. The axial force in these bars takes the value

$$N_2 = 4\Omega E \frac{1}{a} \cos^2 \alpha 1.5625 \frac{a\sigma_Y}{E} = 3.125\Omega\sigma_Y .$$

The vertical equilibrium condition is then used to compute the corresponding value of P , yielding $P = 8.2097\Omega\sigma_Y$.

We conclude therefore that the load-displacement (P - δ) diagram of this structure has 4 straight line segments. The coordinates of the three corners, which correspond to the yielding of the different bars, are the (P , δ) pairs $(5.9742\Omega\sigma_Y, \frac{a\sigma_Y}{E})$, $(8.2097\Omega\sigma_Y, 1.5625 \frac{a\sigma_Y}{E})$ and $(8.8284\Omega\sigma_Y, 2 \frac{a\sigma_Y}{E})$.

VI.8. In the structure represented in Fig. VI.8-a bars AB and BC may be considered as rigid. The wires BD , EF and AC are made of a ductile material with elastic, perfectly plastic behaviour, with an elasticity modulus E and a yielding stress σ_Y . Determine the yielding sequence of the three wires, when the value of force P is gradually increased from zero until the value which causes the collapse of the structure.

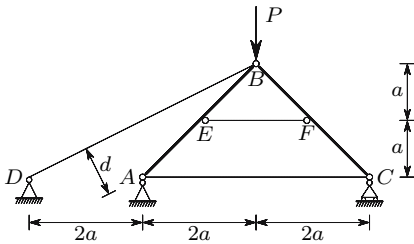


Fig. VI.8-a

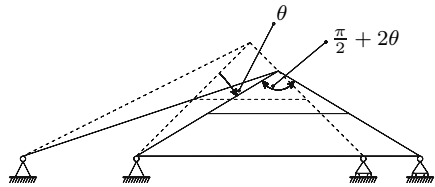


Fig. VI.8-b

Resolution

The degree of kinematic indeterminacy of the structure is one, since once the horizontal displacement of the support C is known, for example, the deformed configuration of the structure is completely defined.

Taking the rotation θ (Fig. VI.8-b) as the kinematic parameter, we get the elongations given below for the wires BD , EF and AC

$$\Delta l_{BD} = \theta \times d = \theta \times 2a \sin \left(\arctan \frac{2a}{4a} \right) = 2 \sin \left(\arctan 0.5 \right) a \theta$$

$$\Delta l_{EF} = 2\theta \times a = 2a\theta$$

$$\Delta l_{AC} = 2\theta \times 2a = 4a\theta .$$

The undeformed lengths of these bars are

$$l_{BD} = 2\sqrt{5}a \quad l_{EF} = 2a \quad l_{AC} = 4a .$$

The corresponding strains are then

$$\varepsilon_{BD} = \frac{2 \sin \left(\arctan 0.5 \right) a \theta}{2\sqrt{5}a} = 0.2 \theta \quad \varepsilon_{EF} = \frac{2a\theta}{2a} = \theta \quad \varepsilon_{AC} = \frac{4a\theta}{4a} = \theta .$$

We conclude that the wires EF and AC yield at the same time for a value $\theta = \varepsilon_Y = \frac{\sigma_Y}{E}$. Yielding of bar DB takes place only for $\theta = 5\varepsilon_Y$.

VI.9. In the structure represented in Fig. VI.9-a the horizontal bar may be considered as rigid. The inclined bars have different cross-section areas and are made of a material with elastic, perfectly plastic behaviour. Determine the yielding sequence of the inclined bars when the value of force P is gradually increased from zero until the value which causes the collapse of the structure.

Resolution

As in example VI.8, we have a structure with a degree of kinetic indeterminacy one, so that the elongation in each inclined bar may be directly related to the kinematic parameter. The cross-section areas do not play any role in that relation nor, as a consequence, in the bars' yielding sequence.

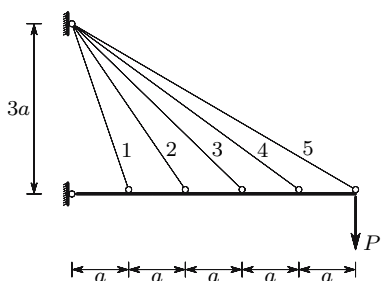


Fig. VI.9-a

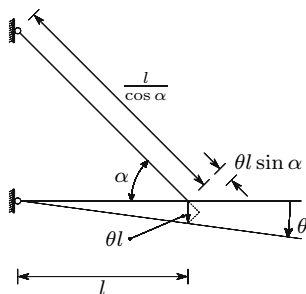


Fig. VI.9-b

Taking the rotation θ (Fig. VI.9-b) as kinematic parameter, the strain in a generic bar whose position is defined by the distance l from the support takes the value

$$\varepsilon = \frac{\theta l \sin \alpha}{\frac{l}{\cos \alpha}} = \theta \sin \alpha \cos \alpha = \frac{\sin 2\alpha}{2} \theta .$$

Particularizing this expression for each of the five inclined bars, we get

$$\begin{aligned} \text{bar 1: } l = a &\Rightarrow \alpha = \arctan \frac{3a}{a} \Rightarrow \varepsilon = 0.3 \theta \\ \text{bar 2: } l = 2a &\Rightarrow \alpha = \arctan \frac{3a}{2a} \Rightarrow \varepsilon \approx 0.46154 \theta \\ \text{bar 3: } l = 3a &\Rightarrow \alpha = \arctan \frac{3a}{3a} \Rightarrow \varepsilon = 0.5 \theta \\ \text{bar 4: } l = 4a &\Rightarrow \alpha = \arctan \frac{3a}{4a} \Rightarrow \varepsilon = 0.48 \theta \\ \text{bar 5: } l = 5a &\Rightarrow \alpha = \arctan \frac{3a}{5a} \Rightarrow \varepsilon \approx 0.44118 \theta . \end{aligned}$$

The yielding sequence of the inclined bars is defined by the descending order of these strains, i.e., $3 \rightarrow 4 \rightarrow 2 \rightarrow 5 \rightarrow 1$.

VI.10. The bar \overline{AB} of the structure represented in Fig. VI.10 is sufficiently stiff to be considered as rigid. The vertical bars are made of a brittle material with linear elastic behaviour until rupture defined by a Young's modulus E and a rupture stress σ_r .

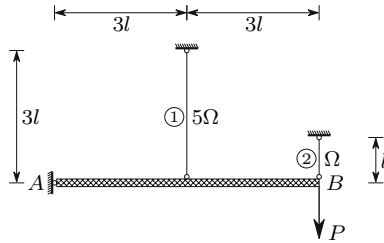


Fig. VI.10

- Determine the value of P which causes the collapse of the structure.
- Determine the increase in loading capacity that can be obtained by prestressing the structure, so that the two vertical bars reach the rupture stress simultaneously.
- Assuming that the prestressing is achieved by fabricating bar 1 with a length which is slightly different from the design length $3l$ and denoting by $3l + l_r$ the undeformed length of this bar, determine the value of l_r which maximizes the loading capacity of the structure.
- Ascertain whether the structure resists the initial internal forces ($P = 0$) caused by the prestressing. If it does not resist, compute the minimum value of force P .

Resolution

The equilibrium condition of moments in relation to point A yields the relation

$$6lP = 3lN_1 + 6lN_2 \Rightarrow P = \frac{N_1}{2} + N_2 .$$

Since the degree of kinematic indeterminacy is one, an infinitesimal rotation of the rigid bar around point A yields the condition of deformation compatibility of the vertical bars

$$\Delta l_1 = \frac{\Delta l_2}{2} \Rightarrow \varepsilon_2 = 6\varepsilon_1 .$$

(a) The axial forces in the vertical bars may be computed from the previous two conditions. The relations between the axial forces and the strains in the two vertical bars are

$$\varepsilon_1 = \frac{N_1}{E5\Omega} \quad \text{and} \quad \varepsilon_2 = \frac{N_2}{E\Omega} .$$

Substituting these values in the compatibility relation, we get

$$N_1 = \frac{5}{6}N_2 .$$

This equation and the equilibrium condition define a system of two equations, whose solution yields the axial forces and the stresses

$$\begin{cases} N_1 = \frac{10}{17}P \\ N_2 = \frac{12}{17}P . \end{cases} \Rightarrow \begin{cases} \sigma_1 = \frac{N_1}{5\Omega} = \frac{2}{17} \frac{P}{\Omega} \\ \sigma_2 = \frac{N_2}{\Omega} = \frac{12}{17} \frac{P}{\Omega} . \end{cases}$$

The rupture of bar 2 occurs at first and takes place when force P reaches the value

$$\sigma_2 = \sigma_r \Rightarrow P = \frac{17}{12}\Omega\sigma_r .$$

The rupture of this bar does not cause the collapse of the structure, since bar 1 alone is able to support this value of P , as may be easily verified from the equilibrium condition with $N_2 = 0$

$$N_1 = 2P = \frac{34}{12}\Omega\sigma_r \Rightarrow \sigma_1 = \frac{N_1}{5\Omega} = \frac{17}{30}\sigma_r < \sigma_r .$$

(The dynamic effects associated with the shock caused by the rupture of a bar on the other structural elements is not considered here. The study of this kind of problem is introduced in Chap. XII). The value of P which causes the rupture of bar 1 and, as a consequence, the structural failure is then

$$\sigma_1 = \sigma_r \Rightarrow \frac{2P}{5\Omega} = \sigma_r \Rightarrow P = \frac{5}{2}\Omega\sigma_r = 2.5\Omega\sigma_r .$$

- (b) The loading corresponding to the simultaneous rupture of the two bars in the prestressed structure may be obtained directly from the equilibrium condition and takes the value

$$\begin{cases} N_1 = 5\Omega\sigma_r \\ N_2 = \Omega\sigma_r \end{cases} \Rightarrow P = \frac{1}{2}5\Omega\sigma_r + \Omega\sigma_r = 3.5\Omega\sigma_r .$$

We find that, prestressing the structure, its loading capacity may be increased by 40%.

- (c) The value of l_r which introduces the optimum residual forces may be obtained by considering it as a residual deformation in the constitutive law of the material of bar 1. Under these conditions, the stress-strain relation in this bar takes the form

$$\varepsilon_1 = \frac{l_r}{3l} + \frac{\sigma_1}{E} .$$

Substituting this value in the condition of compatibility in terms of strains and considering $\sigma_1 = \sigma_2 = \sigma_r$, we get

$$\varepsilon_2 = 6\varepsilon_1 \Rightarrow \frac{\sigma_r}{E} = 6 \left(\frac{l_r}{3l} + \frac{\sigma_r}{E} \right) \Rightarrow l_r = -\frac{5}{2} \frac{l\sigma_r}{E} .$$

We conclude that, in order to have a simultaneous rupture of the two bars, the undeformed length of bar 1 must be $l_1 = 3l - 2.5 \frac{l\sigma_r}{E}$.

- (d) The axial forces in the vertical bars under the actions of the prestressing internal forces and load P may be computed by introducing the value of l_r into the compatibility condition, which yields

$$\varepsilon_2 = 6\varepsilon_1 \Rightarrow \frac{N_2}{E\Omega} = 6 \left(\frac{N_1}{E5\Omega} - \frac{5}{2} \frac{l\sigma_r}{E} \frac{1}{3l} \right) \Rightarrow \frac{6}{5}N_1 - N_2 = 5\Omega\sigma_r .$$

Solving the system formed by this equation and the equilibrium condition, we get the axial forces

$$N_1 = \frac{10}{17}P + \frac{50}{17}\Omega\sigma_r \quad \text{and} \quad N_2 = \frac{24}{34}P - \frac{50}{34}\Omega\sigma_r .$$

The residual stresses are the stresses corresponding to $P = 0$, taking the values

$$P = 0 \Rightarrow \begin{cases} N_1 = \frac{50}{17}\Omega\sigma_r \\ N_2 = -\frac{50}{34}\Omega\sigma_r \end{cases} \Rightarrow \begin{cases} \sigma_1 = \frac{N_1}{5\Omega} = \frac{10}{17}\sigma_r \\ \sigma_2 = \frac{N_2}{\Omega} = -\frac{50}{34}\sigma_r \approx -1.47\sigma_r . \end{cases}$$

We conclude that bar 2 does not resist the initial internal forces, since for $P = 0$ the stress exceeds the rupture stress. The minimum load necessary for the internal force in bar 2 not to exceed its strength, is then

$$\sigma_2 = -\sigma_r \Rightarrow N_2 = \frac{24}{34}P - \frac{50}{34}\Omega\sigma_r = -\Omega\sigma_r \Rightarrow P = \frac{2}{3}\Omega\sigma_r \approx 0.19P_{\max} .$$

VI.11. In the symmetrical structure depicted in Fig. VI.11-a the bending stiffness of the horizontal bar is sufficiently high to consider the bar as rigid. The vertical bars are cables made of a material with linear elastic behaviour until rupture, defined by a modulus of elasticity E and a rupture stress σ_r . In order to optimize the loading capacity of the structure, the middle cable is slightly longer than the design length l . Compute the exact undeformed length of this cable, so that the three cables reach rupture stress at the same time.

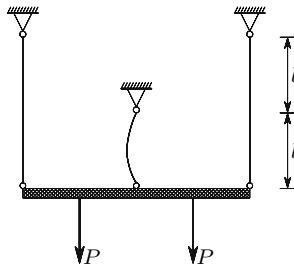


Fig. VI.11-a

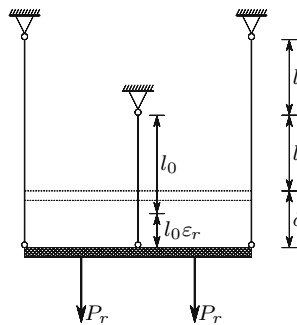


Fig. VI.11-b

Resolution

As the cables are made of the same material, they must have the same strain $\varepsilon_r = \frac{\sigma_r}{E}$ at the moment of structural collapse. The lateral cables reach the rupture strain, when the vertical displacement of the rigid bar attains the value

$$\delta = 2l\varepsilon_r = 2l\frac{\sigma_r}{E} .$$

The situation of simultaneous rupture of the three cables is depicted in Fig. VI.11-b. Denoting the undeformed length of the middle cable by l_0 , this value may be obtained by the following equation

$$\delta = 2l\varepsilon_r = l_0 + l_0\varepsilon_r - l \Rightarrow l_0 = \frac{1 + 2\frac{\sigma_r}{E}}{1 + \frac{\sigma_r}{E}}l .$$

VI.12. Consider a homogeneous vertical prismatic bar supported in its bottom cross-section, under its self-weight. The bar has height h and is made of an isotropic material with linear elastic behaviour. Disregarding the end effect introduced by the support, i.e., considering only the part of the bar which is sufficiently far from the support to accept the validity of Saint-Venant's principle, show that a uniform stress distribution in the cross-sections obeys every condition of equilibrium and compatibility.

Resolution

Considering a reference frame with the axes x and y in the horizontal plane containing the upper cross-section of the bar and axis z pointing from top to bottom, the assumed stress distribution corresponds to the following components of the stress tensor

$$\sigma_x = \sigma_y = \tau_{xy} = \tau_{xz} = \tau_{yz} = 0 \quad \text{and} \quad \sigma_z = -qz ,$$

where q represents the weight of the material per unit of volume.

We conclude at once that the differential equations of equilibrium (5) are satisfied, since the only body force is $Z = q$.

We also easily verify that the conditions of equilibrium at the boundary (8) are satisfied at the upper cross-section (in this section both the stresses and the boundary forces vanish) and at the lateral boundary (in this surface we have $\sigma_z \neq 0$ but also $n = 0$, so that the product $n\sigma_z$ vanishes). At the bottom cross-section, however, the conditions of equilibrium at the boundary ($\bar{Z} = \sigma_z$, (8) with $l = m = 0$ and $n = 1$) are only satisfied if the reaction force is uniformly distributed on the contact surface ($\bar{Z} = -qh$). Generally this does not happen, since in order to have this stress distribution, the support would have to deform in the same way as the bar at the bottom cross-section with the assumed stress distribution (it may be shown that the cross-sections take a spherical shape). However, in accordance with Saint-Venant's principle, we may assume a uniform stress distribution if we consider only points which are not close to this section.

With respect to the equations of strain compatibility, only (53) have to be considered if the bar is simply-connected, i.e., if the cross-section does not have holes. From Hooke's law for isotropic materials (74) and (75) we get the strain functions in the bar, which take the forms

$$\varepsilon_x = \varepsilon_y = -\frac{\nu}{E}\sigma_z = \frac{\nu q}{E}z \quad \varepsilon_z = \frac{1}{E}\sigma_z = -\frac{q}{E}z \quad \gamma_{xy} = \gamma_{xz} = \gamma_{yz} = 0 .$$

We conclude immediately that the equations of strain compatibility are satisfied, since these expressions are linear, which means that their second derivatives are zero (74) and (75) contain only second derivatives of the strain functions).

Since the bar is statically determinate, in terms of the way as it is supported, it is not necessary to verify whether the displacements are compatible with the support conditions (which would be an integral condition of compatibility). Thus, the assumed stress distribution obeys all conditions of equilibrium and compatibility. According to the Theorem of Uniqueness (cf. e.g. [2]) the linear problems of Continuum Solid Mechanics (materials obeying the Hooke's law and linear strain displacement relations) admit only one solution. This means that the assumed stress distribution is the actual solution of the problem.

VI.13. Obtain Expression 133 by means of the force method.

Resolution

Let us first consider that, in order to get a statically determined base structure, the connection between the two materials is released and that the axial force N is a tensile one and is applied to the part of the bar made of material a . Under these conditions, only the part of the bar which is made of material a is deformed. The corresponding elongation takes the value

$$\Delta l = \frac{Nl}{E_a \Omega_a},$$

where l represents the length of the bar. This deformation introduces a discontinuity in the cross-sections of the bar, which must be eliminated. To this end, let us consider a tensile axial force N' acting on the part of the bar made of material b and a compressive axial force with the same value N' acting on the part of the bar made of material a . Since this pair of forces has a zero resultant, it does not affect the total axial force considered in the first step. The pair of axial forces N' , which represents the hyperstatic unknown, causes the deformations

$$\Delta l'_a = \frac{N'l}{E_a \Omega_a} \quad (\text{shortening}) \quad \text{and} \quad \Delta l'_b = \frac{N'l}{E_b \Omega_b} \quad (\text{elongation}).$$

The discontinuity in the cross-sections of the bar is eliminated if $\Delta l'_a + \Delta l'_b = \Delta l$. This condition defines an equation, from which the value of the hyperstatic unknown may be obtained, yielding

$$\Delta l = \Delta l'_a + \Delta l'_b \Rightarrow \frac{Nl}{E_a \Omega_a} = \frac{N'l}{E_a \Omega_a} + \frac{N'l}{E_b \Omega_b} \Rightarrow N' = \frac{NE_b \Omega_b}{E_a \Omega_a + E_b \Omega_b}.$$

The stresses in each material are then

$$\sigma_a = \frac{N - N'}{\Omega_a} = \frac{NE_a}{E_a\Omega_a + E_b\Omega_b} \quad \text{and} \quad \sigma_b = \frac{N'}{\Omega_b} = \frac{NE_b}{E_a\Omega_a + E_b\Omega_b} .$$

The axial force N' is the resultant of the tangential stresses appearing in the connection between the two materials, when the axial force is applied in only one of the them. By means of the Saint-Venant's principle, it can be easily proved that these stresses appear only near to the cross-section where the external forces are applied and that they are independent of the length of the bar.

VI.14. Generalize (133) to a composite prismatic bar made of n materials.

Resolution

Since the degree of static indeterminacy is $n - 1$ and the degree of kinematic indeterminacy is 1, it is more convenient to use the displacement method.

As the strain is the same in all materials, the stresses in each of them may be expressed as functions of the stress in one of them. Thus, we have

$$\varepsilon = \frac{\sigma_i}{E_i} = \frac{\sigma_j}{E_j} \Rightarrow \sigma_i = \frac{\sigma_j}{E_j} E_i .$$

The condition of static equilibrium requires that the resultant of the stresses is equal to the axial force. Thus, we must have

$$N = \sum_{i=1}^n \sigma_i \Omega_i .$$

Expressing all the stresses σ_i as functions of the stress σ_j and substituting in the previous expression, we get the stress in material j

$$N = \frac{\sigma_j}{E_j} \sum_{i=1}^n E_i \Omega_i \Rightarrow \sigma_j = \frac{NE_j}{\sum_{i=1}^n E_i \Omega_i} .$$

VI.15. Figure VI.15-a represents the cross-section of a bar made of two materials, whose constitutive laws are defined by the stress-strain diagrams presented in Fig. VI.15-b.

- Compute the maximum axial force that may be applied to the bar with the two materials in the elastic regime.
- Compute the axial force which causes yielding of the bar.
- In order to maximize the tensile loading capacity of the bar with both materials in the elastic regime, the bar is prestressed, by applying a tensile axial force to the interior part of the bar (material *a*) before the connection between the two materials is established. This force is removed after the connection's bonding.

Compute the value of the prestressing axial force, which leads to the simultaneous yielding of the two materials.

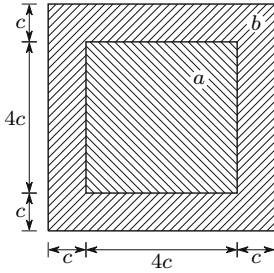


Fig. VI.15-a

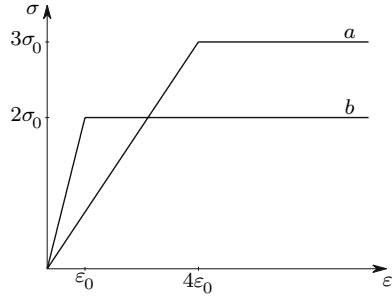


Fig. VI.15-b

Resolution

The areas occupied by each material in the cross-section and the elasticity moduli of the two materials take the values

$$\Omega_a = (4c)^2 = 16c^2; \quad \Omega_b = (6c)^2 - 16c^2 = 20c^2; \quad E_a = \frac{3\sigma_0}{4\varepsilon_0}; \quad E_b = \frac{2\sigma_0}{\varepsilon_0} .$$

- (a) The maximum strain with both materials in the elastic regime is the yielding strain of material *b*, $\varepsilon = \varepsilon_0$, as is easily concluded from the stress-strain diagrams (Fig. VI.15-b). The stresses corresponding to this strain in the two materials are

$$\sigma_a = \varepsilon_0 E_a = \frac{3}{4}\sigma_0 \quad \text{and} \quad \sigma_b = 2\sigma_0 .$$

The axial force resulting from these stresses is then

$$N = \sigma_a \Omega_a + \sigma_b \Omega_b = \frac{3}{4}\sigma_0 \times 16c^2 + 2\sigma_0 \times 20c^2 = 52\sigma_0 c^2 .$$

- (b) When the bar yields, the stresses in the two materials are the corresponding yielding stresses. Thus the yielding axial force of this bar takes the value

$$N = \sigma_a \Omega_a + \sigma_b \Omega_b = 3\sigma_0 \times 16c^2 + 2\sigma_0 \times 20c^2 = 88\sigma_0 c^2 .$$

- (c) The prestressing force must take a value that leads to a strain in material *b* with the value $\varepsilon_b = \varepsilon_0$, when the strain in material *a* takes the value $\varepsilon_a = 4\varepsilon_0$. As at the moment of application of the prestressing force we have $\sigma_b = 0 \Rightarrow \varepsilon_b = 0$, the strain needed in material *a* at the same time is

$$\varepsilon_a = 3\varepsilon_0 \Rightarrow \sigma_a = E_a \varepsilon_a = \frac{3}{4} \frac{\sigma_0}{\varepsilon_0} \times 3\varepsilon_0 = \frac{9}{4}\sigma_0 .$$

The force which introduces the required prestressing is then

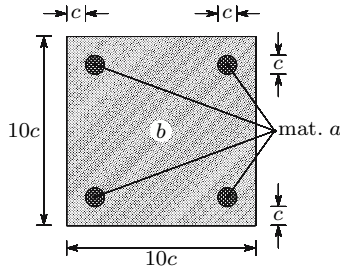


Fig. VI.16

$$N = \sigma_a \Omega_a = \frac{9}{4} \sigma_0 \times 16c^2 = 36\sigma_0 c^2 .$$

This prestressing force raises the maximum load in the elastic regime from $52\sigma_0 c^2$ to the yielding stress of the bar ($88\sigma_0 c^2$).

VI.16. Figure VI.16 shows the cross-section of a prismatic bar made of two materials, a and b , with linear elastic behaviour until rupture. The elasticity moduli and the rupture stresses of the two materials take the values

$$\begin{cases} E_a = 30E \\ E_b = E \end{cases} \quad \begin{cases} \sigma_{ra} = 150\sigma_r \\ \sigma_{rb} = \sigma_r . \end{cases}$$

- Disregarding dynamic effects compute the value of the tensile axial force which causes the rupture of each material.
- In order to maximize the tensile axial loading capacity, the bar is prestressed. The prestressing residual forces are introduced by applying a tensile axial force to each of the bars of material a before the connection between the two materials is established. These forces are removed after the two materials are bonded together.

Compute the force to be applied to each bar of material a , in order to obtain a simultaneous rupture of the two materials under a tensile axial force applied to the composite bar.

- Under the conditions specified in question b), compute the value of the tensile axial force which causes the rupture of the bar.
- Under the conditions specified in question b), compute the stresses in the two materials, when the axial force is zero.

Resolution

- The areas occupied by each material and the corresponding rupture strains take the values

$$\Omega_a = \pi c^2 \quad \Omega_b = (100 - \pi) c^2 \quad \varepsilon_{ra} = 5 \frac{\sigma_r}{E} \quad \varepsilon_{rb} = \frac{\sigma_r}{E} .$$

Since the strain is constant in the cross-section, material b reaches the rupture strain at first. This rupture takes place when the stresses take the values

$$\varepsilon = \frac{\sigma_r}{E} \Rightarrow \begin{cases} \sigma_a = E_a \varepsilon = 30E \frac{\sigma_r}{E} = 30\sigma_r \\ \sigma_b = E_b \varepsilon = E \frac{\sigma_r}{E} = \sigma_r . \end{cases}$$

The axial force which causes rupture of material b is then

$$\begin{aligned} N &= \sigma_a \Omega_a + \sigma_b \Omega_b = 30\sigma_r \pi c^2 + \sigma_r (100 - \pi) c^2 \\ &= (29\pi + 100) c^2 \sigma_r \approx 191.106 c^2 \sigma_r . \end{aligned}$$

Since dynamic effects may be ignored, this axial force does not cause the rupture of the bar. In fact, when the value of the axial force exceeds this value, material b ceases to contribute to the resistance of the bar, but material a only attains its rupture stress, when the axial force reaches the value

$$N = \Omega_a \sigma_{ra} = \pi c^2 150 \sigma_r \approx 471.239 c^2 \sigma_r .$$

- (b) In order to achieve the simultaneous rupture of the two materials, material a must already have a strain $\varepsilon_a = 4 \frac{\sigma_r}{E}$, when the strain in material b is zero. In this way, when the strain in the cross-section increases $\varepsilon_{rb} = \frac{\sigma_r}{E}$, we will have $\varepsilon_b = \frac{\sigma_r}{E}$ and $\varepsilon_a = 5 \frac{\sigma_r}{E} = \varepsilon_{ra}$. The force needed to introduce the required prestressing, i.e. to introduce the strain $\varepsilon_a = 4 \frac{\sigma_r}{E}$ into a bar of material a , then takes the value

$$N = \varepsilon_a E_a \frac{\Omega_a}{4} = 4 \frac{\sigma_r}{E} 30E \frac{\pi c^2}{4} = 30\pi c^2 \sigma_r \approx 94.248 c^2 \sigma_r .$$

- (c) Since, under the conditions defined in the previous answer, the rupture of both materials occurs for the same strain, the tensile axial force to rupture the bar takes the value

$$\begin{aligned} N &= \sigma_{ra} \Omega_a + \sigma_{rb} \Omega_b \\ &= 150\sigma_r \pi c^2 + \sigma_r (100 - \pi) c^2 = (100 + 149\pi) c^2 \sigma_r \approx 568.097 c^2 \sigma_r . \end{aligned}$$

We conclude that the residual forces introduced by the prestressing procedure increase the tensile loading capacity of the bar from $471.239 c^2 \sigma_r$ to $568.097 c^2 \sigma_r$.

- (d) Taking as reference the strain in material b , the constitutive laws of the two materials are defined by the expressions below (note that, when the strain in material b is zero, the stress in material a is $\sigma_a = 4 \frac{\sigma_r}{E} 30E = 120\sigma_r$)

$$\sigma_a = 120\sigma_r + 30E\varepsilon \quad \text{and} \quad \sigma_b = E\varepsilon .$$

The strain corresponding to a zero axial force may be computed from the condition

$$\begin{aligned}
 N = \sigma_a \Omega_a + \sigma_b \Omega_b = 0 &\Rightarrow (120\sigma_r + 30E\varepsilon) \pi c^2 + E\varepsilon (100 - \pi) c^2 = 0 \\
 \Rightarrow \varepsilon &= -\frac{120\pi}{100 + 29\pi} \frac{\sigma_r}{E}.
 \end{aligned}$$

The stresses corresponding to this strain in each material are then

$$\begin{aligned}
 \sigma_a = E_a \varepsilon = 120\sigma_r + 30E \left(-\frac{120\pi}{100 + 29\pi} \frac{\sigma_r}{E} \right) &\approx 60.820 \sigma_r \\
 \sigma_b = E_b \varepsilon = E \left(-\frac{120\pi}{100 + 29\pi} \frac{\sigma_r}{E} \right) &\approx -1.973 \sigma_r.
 \end{aligned}$$

These stresses could also be computed by means of the superposition principle, taking the stresses acting in the situation defined in question b) ($\sigma_a = 120\sigma_r$ and $\sigma_b = 0$) and adding to them the stresses caused by the elimination of the axial force, i.e., by a compressive axial force $N = -\sigma_a \Omega_a = -120\pi c^2 \sigma_r$. These stresses could be computed by means of (133).

Note that the absolute value of the initial strain obtained for material b exceeds its tensile strength. If the material has the same rupture stress for tensile and compressive forces, it will be necessary to have a minimum tensile axial force, in order to prevent this material from failing under the action of the prestressing forces. However, brittle materials usually have a much higher strength in compression than under tensile forces.

This example describes a prestressing technique widely used in prefabricated concrete structural elements called *pre-tensioning*. Another technique called *post-tensioning* is more used in on-site prestressing, once the structure is built. In this technique channels are left in the concrete element, where the prestressing steel wires are introduced later. The prestressing forces in these wires are usually introduced by means of hydraulic jacks which are supported by the concrete element to be prestressed itself. In this situation the reaction forces of the jacks are transmitted to the concrete element, so that the total axial force is zero. In this situation, the axial force to be applied to the prestressing wire is lower, corresponding to the stress computed in answer d). In the present example, the force to be applied in each bar of material a would be $N = 60.82 \sigma_r \frac{\pi c^2}{4} = 47.768 c^2 \sigma_r$.

VI.17. Determine the displacement of the cross-sections of a vertical cable with length l and cross-section area Ω , supported in its upper end, under the action of its self-weight and of a downwards vertical force P applied in its bottom cross-section.

Resolution

Let us consider a vertical coordinate z originating in the bottom end of the cable and pointing upwards. Denoting by q the self-weight of the cable per unit length, the distribution of the axial force is defined by the expression

$$N = P + qz .$$

The displacement of the cross-section at the distance z from the bottom end may be computed by integrating the elongation of the infinitesimal pieces of length dz' ($z' \equiv z$), between that section and the upper end (137), yielding

$$\Delta l(z) = \frac{1}{E\Omega} \int_z^l (P + qz') dz' = \frac{P}{E\Omega}(l - z) + \frac{q}{2E\Omega}(l^2 - z^2) .$$

The displacement of the bottom end of the cable is then

$$z = 0 \Rightarrow \Delta l = \frac{1}{E\Omega} \left(Pl - \frac{ql^2}{2} \right) .$$

VI.18. Determine the longitudinal shape of a bar with square cross-section, with a vertical axis, under the action of a force P and of its self-weight q per volume unit, as represented in Fig. VI.18-a, in order to have the same stress σ in the whole bar.

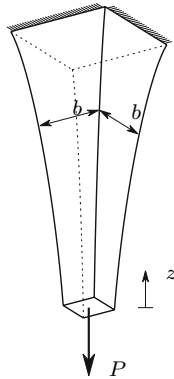


Fig. VI.18-a

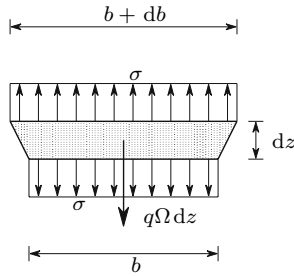


Fig. VI.18-b

Resolution

The condition of equilibrium of the vertical forces acting in a piece of bar with an infinitesimal length dz (Fig. VI.18-b, $\Omega = b^2$) yields the equation

$$\begin{aligned} \sigma\Omega + q\Omega dz &= \sigma(\Omega + d\Omega) \\ \Rightarrow \sigma d\Omega &= q\Omega dz \\ \Rightarrow \sigma \frac{d\Omega}{\Omega} &= q dz . \end{aligned}$$

This differential equation is easily integrated, yielding

$$\sigma \ln \Omega = qz + C \Rightarrow \ln \Omega = \frac{qz + C}{\sigma} \Rightarrow \Omega = C' e^{\frac{qz}{\sigma}} \quad \text{with} \quad C' = e^{\frac{C}{\sigma}} .$$

As the bottom cross-section ($z = 0$) only has to resist to the load P , this cross-section has the area

$$z = 0 \Rightarrow \Omega = \frac{P}{\sigma} .$$

The integration constant and the value of b as function of z are then

$$C' = \frac{P}{\sigma} \Rightarrow \Omega = \frac{P}{\sigma} e^{\frac{qz}{\sigma}} \Rightarrow b = \sqrt{\Omega} = \sqrt{\frac{P}{\sigma}} e^{\frac{qz}{2\sigma}} .$$

We find that the cross-section area grows exponentially with the length of the bar (Fig. VI.18-a). However, the growth rate is very low for the usual structural materials, since the number representing q is generally much smaller than the number representing σ , so that the numerical value of $e^{\frac{qz}{2\sigma}}$ is remains very close to 1, even for significant values of the length of the bar. This means that it is perfectly correct to apply the theory of prismatic members to this bar, with variable cross-section.

VI.19. Compute the axial forces in the column represented in Fig. VI.19.

VI.20. Figure VI.20 represents the cross-section of a prismatic bar made of two materials with linear elastic behaviour. The materials, a and b , have elasticity moduli $E_a = 2E$ and $E_b = 5E$ and coefficients of thermal expansion $\alpha_a = 3\alpha$ and $\alpha_b = \alpha$, respectively.

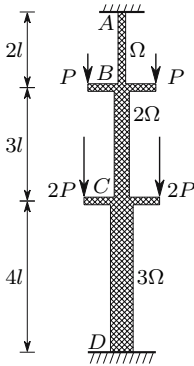


Fig. VI.19

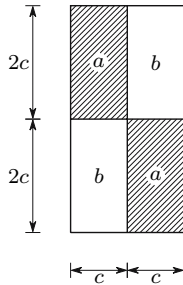


Fig. VI.20

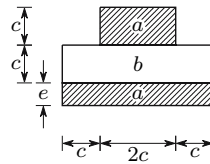


Fig. VI.21

Determine the stresses induced in this cross-section by a temperature rise ΔT . Justify the analytical methodology used.

- VI.21. Figure VI.21 represents the cross-section of a prismatic bar made of two materials, a and b , which have different thermal expansion coefficients. Determine the value of the thickness e , so that a temperature variation does not introduce curvature in the bar.